NAVAL
POSTGRADUATE
SCHOOL

MONTEREY, CALIFORNIA

THESIS

UNCERTAINTY QUANTIFICATION USING EPI-SPLINES AND SOFT INFORMATION

by

Stephen E. Hunt, Jr.

June 2012

Thesis Advisor:	Johannes O. Royset
Second Reader:	Scott T. Nestler

Approved for public release; distribution is unlimited

THIS PAGE INTENTIONALLY LEFT BLANK

REPORT DOCUMENTATION PAGE

Form Approved
OMB No. 0704–0188

1. REPORT DATE *(DD–MM–YYYY)*	2. REPORT TYPE	3. DATES COVERED *(From — To)*
7–6–2012	Master's Thesis	2010-07-06—2012-06-15

4. TITLE AND SUBTITLE

Uncertainty Quantification using Epi-Splines and Soft Information

5a. CONTRACT NUMBER

5b. GRANT NUMBER

5c. PROGRAM ELEMENT NUMBER

6. AUTHOR(S)

Stephen E. Hunt, Jr.

5d. PROJECT NUMBER

5e. TASK NUMBER

5f. WORK UNIT NUMBER

7. PERFORMING ORGANIZATION NAME(S) AND ADDRESS(ES)

Naval Postgraduate School
Monterey, CA 93943

8. PERFORMING ORGANIZATION REPORT NUMBER

9. SPONSORING / MONITORING AGENCY NAME(S) AND ADDRESS(ES)

Department of the Army

10. SPONSOR/MONITOR'S ACRONYM(S)

11. SPONSOR/MONITOR'S REPORT NUMBER(S)

12. DISTRIBUTION / AVAILABILITY STATEMENT

Approved for public release; distribution is unlimited

13. SUPPLEMENTARY NOTES

The views expressed in this thesis are those of the author and do not reflect the official policy or position of the Department of Defense or the U.S. Government. IRB Protocol Number: N/A

14. ABSTRACT

This thesis deals with the problem of measuring system performance in the presence of uncertainty. The system under consideration may be as simple as an Army vehicle subjected to a kinetic attack or as complex as the human cognitive process. Information about the system performance is found in the observed data points, which we call hard information, and may be collected from physical sensors, field test data, and computer simulations. Soft information is available from human sources such as subject-matter experts and analysts, and represents qualitative information about the system performance and the uncertainty present. We propose the use of epi-splines in a nonparametric framework that allows for the systematic integration of hard and soft information for the estimation of system performance density functions in order to quantify uncertainty. We conduct empirical testing of several benchmark analytical examples, where the true probability density functions are known. We compare the performance of the epi-spline estimator to kernel-based estimates and highlight a real-world problem context to illustrate the potential of the framework.

15. SUBJECT TERMS

Uncertainty Quantification (UQ), Nonparametric Density Estimation, Epi-Spline, Soft Information

16. SECURITY CLASSIFICATION OF:			17. LIMITATION OF ABSTRACT	18. NUMBER OF PAGES	19a. NAME OF RESPONSIBLE PERSON
a. REPORT	b. ABSTRACT	c. THIS PAGE			
Unclassified	Unclassified	Unclassified	UU	79	19b. TELEPHONE NUMBER *(include area code)*

i

THIS PAGE INTENTIONALLY LEFT BLANK

UNCERTAINTY QUANTIFICATION USING EPI-SPLINES AND SOFT INFORMATION

Stephen E. Hunt, Jr.
Major, United States Army
B.S., Mathematics, Furman University, 1995
M.S., Operations Research, Florida Institute of Technology, 2002

Submitted in partial fulfillment of the
requirements for the degree of

MASTER OF SCIENCE IN OPERATIONS RESEARCH

from the

NAVAL POSTGRADUATE SCHOOL
June 2012

Author: Stephen E. Hunt, Jr.

Approved by: Johannes O. Royset
                     Thesis Advisor

                     Scott T. Nestler
                     Second Reader

                     Robert F. Dell
                     Chair, Department of Operations Research

THIS PAGE INTENTIONALLY LEFT BLANK

ABSTRACT

This thesis deals with the problem of measuring system performance in the presence of uncertainty. The system under consideration may be as simple as an Army vehicle subjected to a kinetic attack or as complex as the human cognitive process. Information about the system performance is found in the observed data points, which we call hard information, and may be collected from physical sensors, field test data, and computer simulations. Soft information is available from human sources such as subject-matter experts and analysts, and represents qualitative information about the system performance and the uncertainty present. We propose the use of epi-splines in a nonparametric framework that allows for the systematic integration of hard and soft information for the estimation of system performance density functions in order to quantify uncertainty. We conduct empirical testing of several benchmark analytical examples, where the true probability density functions are known. We compare the performance of the epi-spline estimator to kernel-based estimates and highlight a real-world problem context to illustrate the potential of the framework.

THIS PAGE INTENTIONALLY LEFT BLANK

Table of Contents

THIS PAGE INTENTIONALLY LEFT BLANK

List of Figures

THIS PAGE INTENTIONALLY LEFT BLANK

List of Tables

THIS PAGE INTENTIONALLY LEFT BLANK

List of Acronyms and Abbreviations

AAV Amphibious Assault Vehicle
ASA American Statistical Association
AVTB Amphibious Vehicle Test Branch
AWARS Advanced Warfighting Simulation
COMBAT XXI Combined Arms Analysis Tool for the 21st Century
EFV Expeditionary Fighting Vehicle
HAT Habitability Assessment Test
IED Improvised Explosive Device
JDLM Joint Deployment Logistics Model
KL Kullback-Leibler
LSC Lower Semi-Continuous
MSE Mean Squared Error
NPS Naval Postgraduate School
OneSAF One Semi-Automated Forces
SIAM Society for Industrial and Applied Mathematics
UQ Uncertainty Quantification
USMC United States Marine Corps

THIS PAGE INTENTIONALLY LEFT BLANK

Executive Summary

This thesis deals with the problem of measuring system performance in the presence of uncertainty. The basic problem construct is that we have stochastic inputs to a system and, therefore, the output performance measure(s) is stochastic. We seek a quantitative description of the output in terms of a probability density which will quantify the uncertainty about the output in question. We refer to this process as *uncertainty quantification* (UQ).

The system under consideration may be as simple as an Army vehicle subjected to a kinetic attack or as complex as the human cognitive process. Information about the system performance is found in the observed data points, which we call *hard* information, and may be collected from physical sensors, field test data, and computer simulations. *Soft* information is available from human sources such as subject-matter experts and analysts, and represents qualitative information about the system performance and the uncertainty present.

A framework for systematically incorporating hard and soft information in the estimation of probability density functions, regression curves, and in other contexts using epi-splines has been developed by Dr. Roger J-B Wets from the University of California, Davis. We propose the use of this epi-spline framework for the estimation of density functions representing system performance in order to quantify uncertainty. We conduct empirical testing of several benchmark analytical examples where the true probability density functions are known. We compare the performance of the epi-spline estimator to kernel-based estimates and highlight a real-world problem context to illustrate the potential of the approach.

The problem of uncertainty quantification is particularly challenging when small data samples are available from which to estimate the true underlying probability density. The empirical testing in this thesis focuses on small data samples and highlights the use of various sources of soft information. Constraint formulations for the soft information are presented and tested in several example cases. We find that with as few as five data observations, reasonably good density estimates can be produced using the epi-spline estimator.

In comparison to traditional kernel-based, nonparametric density estimates, the epi-spline estimates consistently produce smaller average mean square errors (MSE) over fifty replications. Epi-spline estimates based on five data points and no soft information have average MSEs of 23-48% less than the corresponding kernel estimates. In many cases, even more significant improvements are seen in the variability of the MSE statistics of the epi-spline estimates over the

kernel estimates. We see standard deviation reductions of 88-96% over kernel estimates when no soft information is used. In estimates using two sources of soft information, we see a further reduction in the average MSE of up to 65% and 56% in standard deviation beyond that of the no soft information estimates.

Lastly, we use cognitive performance data from a Habitability Assessment Test (HAT) that tests the impact of waterborne motion exposure on U.S. Marines under various conditions. The unique flexibility of the epi-spline estimator is emphasized to show how issues inherent in real-world testing situations can be mitigated.

Acknowledgements

Thank you to my wife, Heather, and my children, Sylvia, Maecy, Stephen III, and Wilhelmina. Your strong support and many sacrifices over the last two years allowed me to stay focused on the task at hand.

I extend sincere thanks and appreciation to my thesis advisor, Dr. Johannes Royset. The dedication and enthusiasm you display in your work is admirable and inspiring. You have taught me a great deal about how to conduct research, and it truly is an honor and a pleasure to work with you.

The work and involvement of COL Scott Nestler in this thesis effort is at a level that deserves much more credit than "second reader." Sir, you have become a mentor that I greatly respect and I hope that the providence of the Army ensures that our paths cross again one day.

Thank you to Dr. Roger J-B Wets for your many contributions to the field of mathematics. I am honored to be associated with your research work, and I hope this thesis is a helpful contribution.

I appreciate the opportunity the U.S. Army has given me to attend graduate school full-time at NPS. It has been an immensely rewarding experience.

THIS PAGE INTENTIONALLY LEFT BLANK

CHAPTER 1:
INTRODUCTION

Leaders and organizations face many difficult decisions under conditions of uncertainty. Most importantly, the uncertainty surrounding the output from a given system poses a significant challenge to decision makers. The system can be relatively simple such as an Army vehicle or highly complex such as an entire battlefield. Regardless the scale of the system, it is desirable to be able to estimate the present and future system performance using all available information.

However, there often exists uncertainty about the information available and how that information is acted upon by the system under consideration. For example, incomplete situational awareness about present conditions as well as imprecise forecasts about future events create uncertainty. As a result, and along with the complexity of the system itself, there exists uncertainty about the output of the system. The ability of the decision maker to have a clear understanding of what the output uncertainty looks like, i.e., its (joint) probability distribution, shape characteristics, moments, quantiles, tail behavior, etc., can have a significant impact on decisions made and courses of action taken.

As defined by Eldred and Swiler [1], uncertainty quantification (UQ) is "the process of determining the effect of input uncertainties on response metrics of interest." More specifically, UQ deals with estimating the characteristics of the probability distributions of the output from complex systems, which have probabilistic data as input. While this can be addressed reasonably well with traditional statistical methods when large amounts of data are available, decisions are often required based on limited data.

Uncertainty quantification, a field relatively young in name, is also growing in research interest. The American Statistical Association (ASA) and Society for Industrial and Applied Mathematics (SIAM) recently announced a joint effort to create the *Journal on Uncertainty Quantification (JUQ)* [2] with the goal of highlighting the interdisciplinary nature of UQ. Berger et al. define the field in somewhat broader terms:

> uncertainty quantification (UQ) in computational science and engineering has to do with describing the effects of error and uncertainty on results based on simulation and prediction of the behavior of constructed models of phenomena in physics,

biology, chemistry, ecology, engineered sytems, politics, etc. ... Results from mathematical modeling are subject to errors and uncertainty emanating from a variety of sources, including uncertainty in data obtained from experiment and observation; limitations of physical modeling, including uncertain coefficients, approximation, and the need for emulation; problems in computer codes; and the difficulty of combining models into integrated systems.

The description provided above and the timely development of a new journal dedicated to UQ highlight the importance of the research presented in this thesis.

1.1 Motivation and Background

The task of measuring system performance, and quantifying the uncertainty resident in the performance, based on small data samples is a particularly challenging problem. Consider, for example, a military research and development field test situation in which the suvivability of a proposed combat vehicle is being measured. Simulations have been conducted, but stakeholders want to make their decision based on results from real-world field test data. The test will subject a sample of the vehicles to an improvised explosive device (IED) of a given magnitude and, based on some quantitative measure, assign the observation a survivability score.

The challenge is that the sample used for the test will be quite small, maybe only five vehicles. The vehicles are in limited testing production and very expensive. How then do we get an accurate view of the uncertainty about the survivability from only five *hard* data observations? *Hard* information is defined as specific data points compatible with traditional statistical estimation techniques. This hard information is often gathered from physical sensors, test data, and computer simulations.

Because we may not want to make explicit assumptions about the performance measure coming from a particular family of probability distributions, we enter the realm of nonparametric estimation. In this thesis, we focus exclusively on cases where the system performance is described by a probability density function. Hence, we exclude the possibility of, for example, integer-valued performance measures. By utilizing nonparametric means, we maintain flexibility in the design characteristics of the density estimate. This is especially important in the context of small data sets because the assumption of a parametric distribution family imposes many constraints that may not be desirable.

The next question to consider is whether the hard information is all that is known about the behavior of this output variable. In many cases there is at least some amount of information that is known about the output and how the system in question acts on the input. This *soft* information is defined as that which is derived from human sources such as human intelligence, signal intelligence, and the experience of analysts. The soft information is often more qualitative in nature coming from a human understanding of characteristics of the system output.

Engineered systems are often represented using models consisting of differential and algebraic equations. Let $G(\omega)$ be the solution of these equations, or aggregated quantities derived from the solution, for a particular choice ω of parameters in the equations. Since the selection of parameters is often subject to uncertainty due to incomplete knowledge about material properties, applied loads, boundary conditions, and environmental factors, the system performance $\xi = G(\omega)$ is uncertain. For example, in vehicle design [3] the system performance $\xi = G(\omega)$ may give a measure of occupant and structural damage in the case of impact or blast of type ω. Since the strength and location of the blast as well as the material properties would typically be unknown, ω is viewed as a random vector. Consequently, the damage $\xi = G(\omega)$ is also a random vector. Knowledge about the underlying differential and algebraic equations may provide information about the range of G, the monotonicity of the density of ξ, and other factors, which we include as soft information in the estimation problem.

Army simulations such as OneSAF, COMBAT XXI, AWARS, and JDLM model various aspects of complex military operations. Simulations of this kind rely on the specification of numerous input parameters ω, which, after running the simulation, result in an output $\xi = G(\omega)$ that may represent performance metrics such as attrition, enemy losses, and supply level. Since there may be significant uncertainty about the value of the input parameters, the system performance is uncertain and needs to be quantified. Experienced analysts may provide knowledge about the nature of the simulations that can be included as soft information in the estimation of the density of ξ.

The cognitive ability of human and autonomous systems under adverse conditions are often subject to significant uncertainty. Still, analysts need to plan for this uncertainty based on limited data. For example, recent field experiments with U.S. Marines landing on a beach under various degrees of stress and fatigue caused by rough seas and other factors, show significant variability in the Marines' cognitive abilities [4].[1] Since the intensity and duration of waterborne

---

[1]In fact, the referenced field experiment with U.S. Marines is the subject of application presented in Chapter 4.

motion during a military operation are unknown a priori, we view them as a random input ω to a Marine's cognitive process, represented by the function G, which results in a random cognitive performance $\xi = G(\omega)$.

It is critical for planners to know the density of ξ or at least some of its moments to better anticipate required unit strength and support. Clearly, G is not known explicitly, but the density of ξ can be estimated based on field tests of the kind presented in [4]. In this situation, contextual knowledge may provide important soft information that improves the estimates significantly.

There are many real world contexts and situations where the need to quantify the uncertainty of a particular system performance measure will present itself. The examples discussed above are merely illustrative of several interesting application areas. We will not examine cases from all of these example areas. This thesis presents test cases of several simple univariate functions, a more complex engineering example, and a real world application related to the human cognitive domain.

A framework for systematically incorporating hard and soft information in the estimation of probability density functions, regression curves, performance functions, and other quantities, particularly in the context of small data sets, using *epi-splines* has been developed by Dr. Roger J-B Wets from the University of California, Davis. This framework differs significantly from the other main approaches to this estimation problem. As mentioned before, when large^2 sample sizes are available many long-standing statistical estimation techniques taking advantage of the Central Limit Theorem and the Law of Large Numbers can be applied effectively.

In the area of UQ, function approximation through variations of polynomial expansion techniques seems to be the most prevalent method currently being pursued. This approach develops polynomial expansion approximations of the system G and, with these, is then able to estimate the measures of interest concerning the output density based on a priori knowledge of the input variables. Results using this approach have proven quite effective and useful [1]. In fact, when G is smooth, this approach has an exponential rate of convergence [5]. However, when ω becomes a high-dimensional vector of inputs it also becomes quite difficult to construct the polynomial expansion because of the large number of parameters.

In the area of density estimation, there has been seminal work building for decades. The basic

---

[2]The designation of large versus small data sets is somewhat dependent on the context. There is no set rule as to what constitutes one or the other in all circumstances. For the purposes of this thesis, we consider small to be less than thirty and large to be 100 or greater, which leaves open a mid-range of values.

algorithm of nonparametric density estimation was introduced in 1951 [6]. Following that initial development, several key papers were published over the next two decades which developed the theoretical foundation of nonparametric density estimation [7]. It is not until 1978, however, that we see the first practical application of these theoretical methods in a paper concerning risk factors in coronary artery disease [8].

These developments all contribute to what is now the most prevalent method for nonparametric density estimation – the kernel estimator. The basic kernel estimator of a density function is constructed by computing a density function for each observation in the data. The shape characteristics of the individual function at each observation depends on the selection of the kernel function. The most common kernel functions used are the Gaussian, Epanechnikov, triangular, and bi-weight density functions because density functions themselves work quite well as kernel functions [7]. The densities at each point in the support are then aggregated to create the single kernel density estimate. Based on the appropriate selection of a kernel function and weights given to the *sub*-densities at each observation, the aggregated density will integrate to one and qualify as a probability density function. It has also been shown that the kernel estimator is consistent and has good asymptotic properties [7].

1.2 Contributions

This thesis examines the validity and potential of the epi-spline framework for UQ problems and advances the understanding of its application to complex systems using small data sets. The implementation of this framework and the numerical work done is contributing to the development of new model formulations and computational methods. As such, this thesis effort may advance the development of estimation toolboxes, which in the future could be used by analysts and leveraged to support decision makers within the Department of Defense and elsewhere.

1.3 Thesis Organization

Chapter 2 explains in more detail the methodology used in this research. We explain the choice of maximum likelihood estimation for determining the objective function of the estimation problem. The epi-spline framework is discussed in greater detail, and the incorporation of soft information into the estimation problem is explained.

Chapter 3 lays out the formulation and results from the benchmark testing and analysis portion of the research. First, we work through some analytic examples building upon preliminary work done on parameterized probability distributions. There has been significant numerical work

testing the epi-spline framework against known parametric probability distributions. We work to benchmark the performance of the epi-spline framework against two *textbook* functions where the output density can be computed analytically using input data from known parameterized distributions. We test a quadratic case where $\xi = G(\omega) = \omega^2$ and an exponential case where $\xi = G(\omega) = e^{\omega}$. The intent is to illustrate the numerical implementation of the epi-spline framework, compare its estimation properties to that of traditional kernel estimates, and provide some analysis of its consistency and asymptotic characteristics.

Chapter 4 explores a real-world application area for the epi-spline framework. Using field test data from another NPS thesis effort regarding the impact of waterborne motion exposure on cognitive performance, we demonstrate the capability of the epi-spline framework being applied to one of the most common, yet most complex, systems known – the human body.

Chapter 5 concludes the thesis by presenting key findings and commends areas of further research to the community of interest.

CHAPTER 2:
METHODOLOGY

We propose the use of a flexible framework based on *epi-splines*, defined in Section 2.2, for consistent approximation of infinite-dimensional optimization problems arising in density estimation. We seek to estimate the density h of ξ by maximizing the likelihood function of a given sample, $\xi^1, \xi^2, \ldots, \xi^\nu$, subject to constraints derived from soft information such as support bounds, density shape, smoothness, moments, convexity of G, and gradient information about G.

2.1 Maximum Likelihood Density Estimation

We use the maximum likelihood function to determine the objective function of the estimation problem. Suppose that h belongs to a function space $\mathcal{H}$ such as a Polish space. A density estimate h^ν of h using a maximum likelihood criterion is given by

$$h^\nu \in \underset{h}{\arg\max}\{E^\nu[\ln h(\xi)] \mid h \in S^\nu \subset \mathcal{H}\}, \tag{2.1}$$

where $E^\nu[\cdot]$ is the expectation with respect to the empirical distribution P^ν generated by the sample $\xi^1, \ldots, \xi^\nu$,

$$S^\nu = A^\nu \cap \{h \in \mathcal{H} \mid h \geq 0 \text{ a.s.}, \int h(\xi)d\xi = 1\}, \tag{2.2}$$

and A^ν is a constraint set that accounts for soft information. Since we seek a probability density, we restrict the optimization to nonnegative functions that integrate to one. From the general formulation presented above, we now propose to parameterize the problem through a specific construction of the epi-spline framework.

2.2 Exponential Epi-Spline Framework

In the estimation of density functions, the primary approximation tool will be *exponential epi-splines*.[3] Given a sample, $\xi^1, \xi^2, \ldots, \xi^\nu$, the exponential epi-spline estimator of h is given by

$$h^\nu = e^{-s^\nu(\cdot)} \tag{2.3}$$

where $s^\nu : R \to \overline{R} = R \cup \{-\infty, \infty\}$ is an epi-spline. One of the main features of epi-splines is that they are determined by a finite number of parameters. Furthermore, epi-splines are dense in the spaces of continuously differentiable functions, of Lipschitz continuous functions, and of lower semi-continuous (lsc) functions [10]. Unlike the construction of standard splines, however, epi-splines are constructed with a focus on approximation rather than interpolation.

The family of epi-splines of order p is defined as follows [10]:

Given $-\infty \le d_{-1} \le d_0 \le \cdots \le d_N \le d_{N+1} \le \infty$, the family of epi-splines of order p, e-spl$^p([d_{-1}, d_0, d_1, \ldots, d_N, d_{N+1}])$, is the collection of functions $s : R \to \overline{R}$ satisfying:

(i) $s(\xi) = \infty$ for $\xi \in (-\infty, d_{-1}]$ and $\xi \in [d_{N+1}, \infty)$,
(ii) s is p times differentiable on (d_{-1}, d_{N+1}),
(iii) $\forall k = 1, 2, \ldots, N$, $s^{(p)}(\xi) = $ constant for $\xi \in (d_{k-1}, d_k)$,
(iv) $s^{(p)}(\xi) = 0$ for $\xi \in (d_{-1}, d_0)$ and (d_N, d_{N+1}).

Here, we use the notation $s^{(p)}(\cdot)$ to denote the pth derivative of s. We note that the tail segments of the density, (d_{-1}, d_0) and (d_N, d_{N+1}), have one less degree of freedom than the other segments, (d_{k-1}, d_k), $k = 1, \ldots, N$. That is, while (d_{k-1}, d_k) has a constant p^{th} derivative, the tails have a pth derivative equal to zero. The reason for this different treatment is that the tail segments typically do not include data points to support a rational choice of the pth derivative.

Optimization over a family of epi-splines using a maximum likelihood criterion produces the following estimator. Given sample $\xi^1, \ldots, \xi^\nu$, *exponential epi-spline estimator $h^\nu = e^{-s^\nu(\cdot)}$*,

---

[3]The term *epi* comes from the fact that the spline-like functions developed rely on epi-convergence results. The usual framework for dealing with the convergence of optimization problems is minimization and relies on epi-convergence. The *epigraph* of a function $f : X \to \overline{R}$ consists of the set of all points in $X \times R$ that lie on or above the graph of f, i.e., set convergence of epigraphs. [9].

where

$$s^V \in \underset{s}{\operatorname{argmin}} E^V[s(\xi)] \qquad (2.4)$$

$$\text{s.t.} \quad s \ \in \ \text{e-spl}^p([d_{-1}, d_0, d_1, ..., d_N, d_{N+1}])$$

$$\int_{-\infty}^{\infty} e^{-s(\xi)} d\xi \ = \ 1$$

$$s \ \in \ S^V,$$

and S^V represents the set of constraints placed on the problem that are defined by the available soft information.

Now, for the actual construction of the exponential epi-spline estimator we use the fact that there exists a one-to-one correspondence between e-spl$^p([d_{-1}, d_0, d_1, ..., d_N, d_{N+1}])$ and R^{p+N}. There exists a function $c^p : R \to R^{p+N}$ such that every $s \in$ e-spl$^p([d_{-1}, d_0, d_1, ..., d_N, d_{N+1}])$ takes the form

$$s(\xi) = \langle c^p(\xi), \alpha \rangle \qquad (2.5)$$

on $[d_{-1}, d_{N+1}]$ for some unique $\alpha \in R^{p+N}$ and where c^p is a piecewise polynomial of order at most p [10].

We call $\alpha \in R^{p+N}$ the *epi-spline vector*. It contains the parameters we seek to optimize based on the maximum likelihood criterion for a given estimation problem. The size of the vector depends on two things: p – the order of the epi-spline being used, and N – the number of discretizations of the support interval of the density function. This means that the number of parameters in the problem is not only finite, but also controllable to the extent that the order of the epi-spline and the number of discretizations can be chosen deliberately.

We work exclusively with epi-splines of order two, e-spl^2, in this thesis work. We have found this to be a sufficiently rich family of epi-splines for our purposes. To illustrate the relationship between the epi-spline construction and a familiar density, consider the normal density:

$$h(\xi) = \frac{1}{\sigma\sqrt{2\pi}} e^{-(\xi-\mu)^2/(2\sigma^2)} \quad -\infty < \xi < \infty$$

Because of the quadratic terms in the exponent, the epi-spline estimator would require a constant second derivative greater than zero to fully represent the normal density function. To achieve that level of fidelity, an epi-spline of order three, e-spl^3, would be required. However, empirical

9

testing supports that a e-spl^2 can estimate the normal density very well.

Contrast this with the exponential density function:

$$h(\xi) = \begin{cases} \frac{e^{-\xi/\beta}}{\beta} & \text{if } 0 \leq \xi < \infty \\ 0 & \text{elsewhere} \end{cases}$$

In this case, second-order epi-splines are sufficient for fully representing the density function. With ξ appearing in the function only to the first power, the second derivative of the density would be zero. As such, the fact that $s^{(2)}(\xi) = 0$ for e-spl^2 presents no loss of fidelity in the estimate.

Epi-splines of order two, e-spl^2, we use in this work are constructed as follows. Let $s \in$ e-spl$^2([d_{N-1}, d_0, d_1, \ldots, d_N, d_{N+1}])$, where $d_{N-1} = -\infty$, $d_{N+1} = \infty$, and $d_k = d_0 + k\delta$, $k = 1, 2, \ldots, N$, for some $\delta > 0$. Then, for $\xi \in (d_{k-1}, d_k]$ where $k = 1, 2, \ldots, N+1$,

$$s(\xi) \;\; = \;\; s_0 + v_0(\xi - d_0) + \delta \sum_{j=1}^{k-1} \left(\xi - d_j + \frac{\delta}{2} \right) a_j + \frac{1}{2} \left(\xi - d_{k-1} \right)^2 a_k \tag{2.6}$$

and for $\xi \in (d_{-1}, d_0)$,

$$s(\xi) = s_0 - v_0(\xi - d_0),$$

where $s_0 = s(d_0)$, $v_0 = s'(d_0)$, and a_j, for $j = 1, 2, \ldots, N+1$, are the constant values of $s''(\cdot)$.

In the e-spl^2 construction shown above in (2.6), the epi-spline vector α is $(s_0, v_0, a_1, \ldots, a_N)$ and δ refers to the width of the discretization intervals. In our construction, we let δ be a constant width throughout the support of the density estimate. Theoretically, this does not have to be the case. There may be situations where it is advantageous to use discretizations of differing widths in particular areas of the support range.

We estimate the epi-spline vector α through the finite-dimensional problem

$$\alpha^\nu \;\; \in \;\; \underset{\alpha}{\text{argmin}} \sum_{i=1}^{\nu} \langle c^p(\xi^i), \alpha \rangle + \int_{d_{-1}}^{d_{N+1}} e^{-\langle c^p(\xi), \alpha \rangle} d\xi \tag{2.7}$$
$$\text{s.t.} \quad \alpha \in A^\nu \subset R^{p+N},$$

which is equivalent to Equation (2.4) under certain assumptions [10].

Note that the objective function is strictly convex because it is the sum of a linear function with a strictly convex function. As a result, if the feasible region A^v is convex, then the solution α^v will be unique [10]. This, in turn, produces a unique density estimate based on α^v. The advantage of working with a convex optimization problem cannot be underestimated in the practical sense of finding numerical solutions. Also, note that the requirement for the density to integrate to one now appears in the objective function.

The exponential epi-spline estimator then becomes

$$h^v(\xi) = e^{-\langle c^p(\xi), \alpha^v \rangle} \tag{2.8}$$

for $\xi \in (d_{-1}, d_{N+1})$ and $h^v(\xi) = 0$ elsewhere.

We would like for a statistical estimator to be consistent. Let the density $h = e^{-s(\cdot)}$, with $s \in \text{e-spl}^p([d_{-1}, d_0, d_1, ..., d_N, d_{N+1}])$ and epi-spline vector α. If $\{\alpha^v\}_{v=1}^{\infty}$ is a sequence of optimal epi-spline vectors, i.e., those determined by (2.7), for a pairwise independent sample $\xi^1, \xi^2, ..., \xi^v$ from h. Then, $\alpha^v \to \alpha$ and h^v epi-converges to h, as $v \to \infty$, almost surely [10] and h^v is, therefore, a consistent estimator.

2.3 Incorporating Soft Information

The systematic incorporation of soft information into the estimation problem is one of the great strengths of the epi-spline framework. Conceptually, it allows for nearly any information to be accounted for in the estimation of h. The only limitation is the ability to construct a mathematical constraint which implements the nature of the soft information. Several of the constructions currently being explored and implemented are presented below, although, not all of these are used in this thesis work.

2.3.1 Absolutely Continuous Distributions

First and foremost is the knowledge that the density of the output of interest is in fact a continuous distribution. The estimation of the density h of ξ would only be meaningful if a density exists. For example, if G is strictly monotonic, or alternatively, differentiable with $P(\nabla G(\omega) = 0) = 0$, and ω has a probability density, then the distribution of ξ is absolutely continuous.

2.3.2 Support Bounds

Bounds on the support of ξ can sometimes be derived from soft information about the system underlying G and from knowledge about the support of ω. For the sake of illustration, suppose that $G(\omega) = \|x^\omega\|_\infty$, where x^ω is a solution of the differential equation $\dot{x}(t) = f(x(t), \omega)$, $t \in [0, 1]$, with $x(0) = x_0(\omega)$, where both the dynamics and the initial conditions are random. Then, under moderate assumptions $\xi = G(\omega) \leq (1 + \|x_0(\omega)\|)e^K$, where K is a constant related to f. Then, bounds on $x_0(\omega)$ yield an upper bound on ξ that can be incorporated as soft information in (2.8). This bound can be strengthened in the case of a linear differential equation. In terms of construction, the bounds are easily implemented using d_{-1} and d_{N+1}.

2.3.3 Unimodality

It is common for a probability density to be unimodal in its shape. This can be implemented with bounds on the epi-spline vector. Since by definition a pth order epi-spline has a piecewise constant p^{th} derivative, we need only require that particular elements of α are non-negative. Specifically,

$$A^v = \{\alpha = (\alpha_1, \alpha_2, ..., \alpha_{p+N}) \in R^{p+N} \mid \alpha_i \geq 0, \tag{2.9}$$
$$i = p+1, p+2, ..., p+N\}$$

2.3.4 Moment Bounds

If G is known to be convex, then $G(E[\omega])$, through Jensen's inequality, provides a lower bound on $E[\xi]$, which can be used in (2.8). Moreover, if the hard data also includes subgradient information about G, which may be the case when $G(\omega)$ derives from the solution of a boundary value problem of a mechanical system; see for example [11], then soft information about ξ is available through cutting plane approximations of G. Specifically, let $\nabla G(\omega^l)$, $l = 1, 2, ..., v$, be subgradients of G at $\omega^1, \ldots, \omega^v$. Then,

$$\hat{G}(\omega) = \max_{l=1,...,v} \{G(\omega^l) + \langle \nabla G(\omega^l), \omega - \omega^l \rangle\}, \tag{2.10}$$

is a lower bounding function of G.

Consequently, the qth moment $E[\xi^q] \geq E[\hat{G}(\omega)^q]$. Since the right-hand side in this inequality may be computable or at least can be estimated with high accuracy, we can generate lower

12

bounds on moments of ξ for use in (2.7). Specifically, we produce constraints of the form:

$$\int_{d_{-1}}^{d_{N+1}} \xi^q e^{-\langle c^p(\xi), \alpha^v \rangle} d\xi \geq E[\hat{G}(\omega)^q]. \tag{2.11}$$

Similarly, $\hat{G}$ may generate upper bounds on the cumulative distribution function of ξ that can also be incorporated in (2.7).

2.3.5 Gradient Bounds

If G is bijective and continuously differentiable, then gradient information about G provides soft information about the density of ξ. For example, for the univariate case where G is a function from $R \to R$, then the density $h(\xi) = f_\omega(\omega)/G'(\omega)$, where f_ω is the density of ω. Hence, bounds on the derivative of G translates into bounds on the density of ξ. Similar bounds can be constructed in higher dimensions with the derivative replaced by the Jacobian determinant.

2.3.6 Chebyshev Bounds

For any $S \subset \Omega$, where Ω is the probability space of input vectors ω, Chebyshev's inequality gives that $P(S)\inf_{\omega \in S} G(\omega) \leq E[\xi]$ and hence provides lower bounds on the expectation of ξ. The computation of the left-hand side in this inequality is difficult in general. However, if G is a function from $R \to R$ and strictly increasing, then the computation is trivial. Under this assumption, it is also easy to determine the exact values of the cumulative distribution function of ξ at the data points $\xi^1, ..., \xi^v$ as they equate to those of the cumulative distribution function of ω at $\omega^1, ..., \omega^v$. Information of this kind translates into constraints in (2.8).

2.3.7 Kullback-Leibler Divergence

Suppose there was soft information that projected that the density h to be estimated was, in some sense, *close* to a known density function. For example, it could be a qualitative judgement from a subject matter expert that h should have a shape similar to some known density. An upper bound on the distance from the known density can be implemented through the use of the Kullback-Leibler divergence measure. The Kullback-Leibler divergence from density h to density g defined on R is

$$d_{KL}(h||g) = \int_{-\infty}^{\infty} h(\xi) \log \frac{h(\xi)}{g(\xi)} d\xi. \tag{2.12}$$

The soft information $d_{KL}(h||e^{-s(\cdot)}) \leq \kappa$ relative to a known density h is implementable as a

linear constraint for a given constant κ. If $s \in$ e-spl$^p([d_{-1}, d_0, d_1, ..., d_N, d_{N+1}])$, then

$$d_{KL}(h||e^{-s(\cdot)}) = \left\langle \int_{d_{-1}}^{d_{N+1}} c^p(\xi)h(\xi)d\xi, \alpha \right\rangle + \int_{-\infty}^{\infty} (\log h(\xi))h(\xi)d\xi \qquad (2.13)$$

where $\alpha \in R^{p+N}$ is the epi-spline vector of s.

If, in addition, $h = e^{-s^*(\cdot)}$, $s^* \in$ e-spl$^p([d_{-1}, d_0, d_1, ..., d_N, d_{N+1}])$, then

$$d_{KL}(h||e^{-s(\cdot)}) = \left\langle \int_{d_{-1}}^{d_{N+1}} c^p(\xi)h(\xi)d\xi, \alpha - \alpha^* \right\rangle, \qquad (2.14)$$

where α^* is the epi-spline vector of s^* [10].

CHAPTER 3:
BENCHMARK TESTING AND ANALYSIS

The purpose of this chapter is to verify through empirical testing the validity and potential of the proposed epi-spline framework for the applications which have been suggested. We want to show that there is a reasonably good fit of the epi-spline estimate to the true density by visual inspection for randomly generated input data in the given cases. We also want to verify the fit of the epi-spline estimate through analysis of mean squared error (MSE) [7].

We compare the epi-spline and standard kernel estimates visually and in terms of MSE. As kernel estimates represent the most commonly used method of nonparametric density estimation, we propose this as a reasonable comparison from which to gauge the fit of the epi-spline estimate. The kernel estimates used throughout the analysis are computed with Matlab's *ksdensity* function using a Gaussian kernel construction and its default algorithm for the selection of an optimal bandwidth.

In this chapter, we consider several simple analytic cases where the true density of the output is known by way of deliberate construction of the input ω and the function G. We then transition to a slightly more complex example of a structural engineering problem taken from [1]. In this latter case, the true density is not known, but through a known definition of the function G and knowledge of the distributions of the input ω we are able to estimate with high accuracy an asymptotically *true* density through large sampling.

Now, Thompson states strongly in the Preface to *Nonparametric Function Estimation, Modeling, and Simulation* [12] "that we passed diminishing returns in 1-d NDE (nonparametric density estimation) around 1978." Although the numerical examples in this thesis are in fact one-dimensional, this is where testing and analysis of the proposed epi-spline framework must begin.

The numerical work presented is done using Matlab version 7.12.0.635, 64-bit on an Apple MacBook Pro operating on Mac OS X version 10.7.3 with a 2.66 GHz Intel Core i7 quad processor and 8 GB 1067 MHz DDR3 memory. We use Matlab's optimization solver *fmincon* with the following settings: MaxIter = 1000, TolFun = 10^{-9}, TolCon = 10^{-9}.

3.1 Quadratic

Let $\xi = G(\omega) = \omega^2$, where $\omega \sim N(0,1)$. This allows us to compare our results with the true density, a chi-square distribution with one degree of freedom, $\chi^2(1)$, see Figure 3.1. In this case, we know something about how the "system" G acts upon the input data ω and we have quite a bit of soft information concerning ξ. That is, we know $G(\omega) = \omega^2$ will produce only non-negative output. We are able to include this information in the form of support bounds on the output by requiring that the left bound be 0. Additionally, we know that the output will be unimodal; in fact, it is not just unimodal but also decreasing over its support.
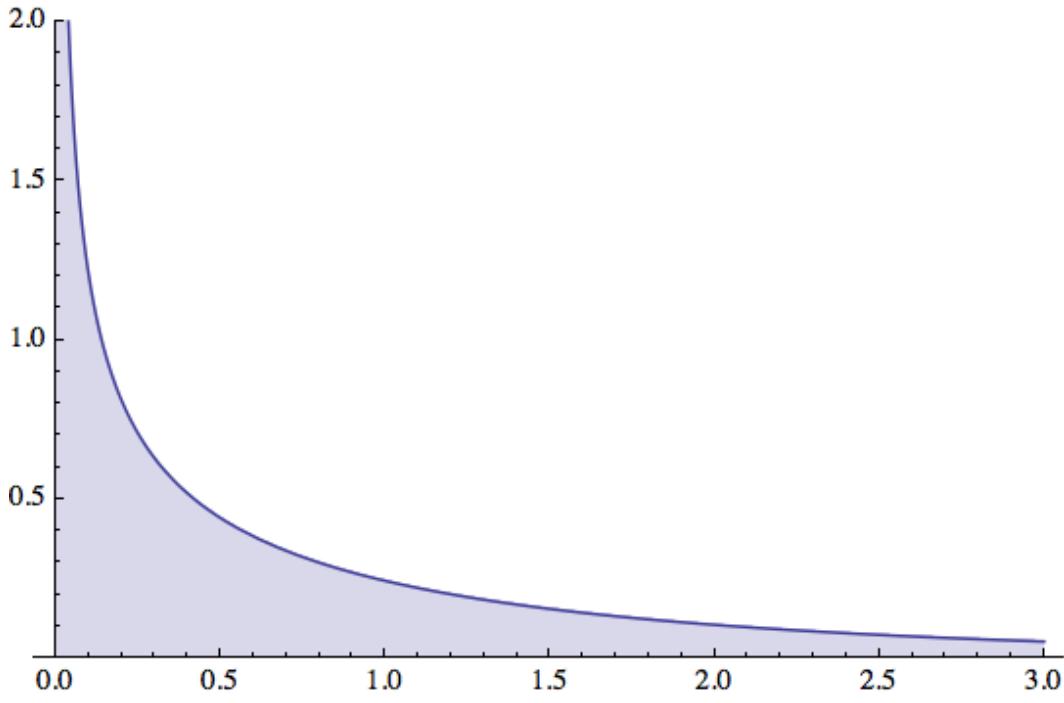

Figure 3.1: $X^2(1)$ density.

3.1.1 Low Information Cases

The first example we present is the estimate of the density of ξ utilizing no soft information. With no soft information, we are limited to estimating the density purely from the data points generated. Figures 3.2 - 3.5 illustrate that the estimated density can take on a wide range of shapes, and this is true for the epi-spline estimate and the kernel estimate. We also see the impact of the sample size. We show estimates based on as many as 100 observations and as few as five. The epi-spline and kernel estimates are much closer in shape when there is a larger sample from which to construct the estimate.
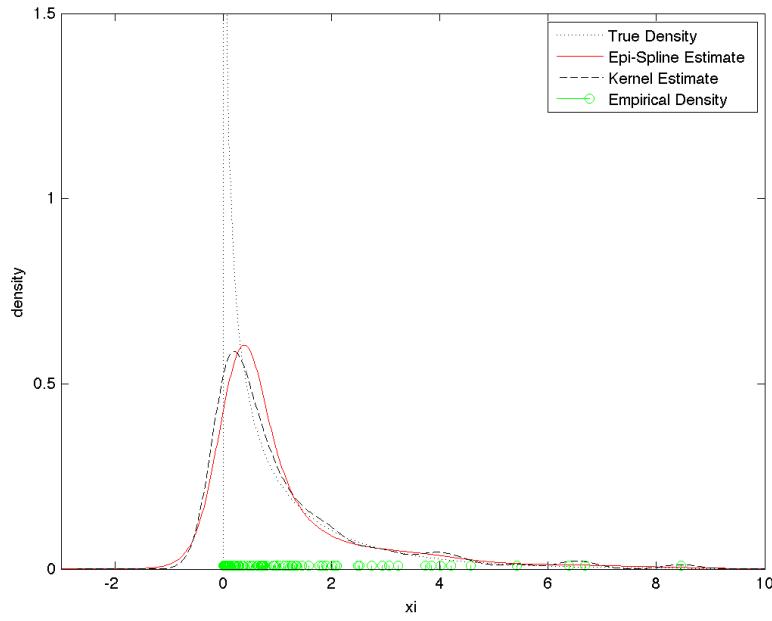
Figure 3.2: Density estimate of $\xi = G(\omega) = \omega^2$ with no soft information and $n = 100$.
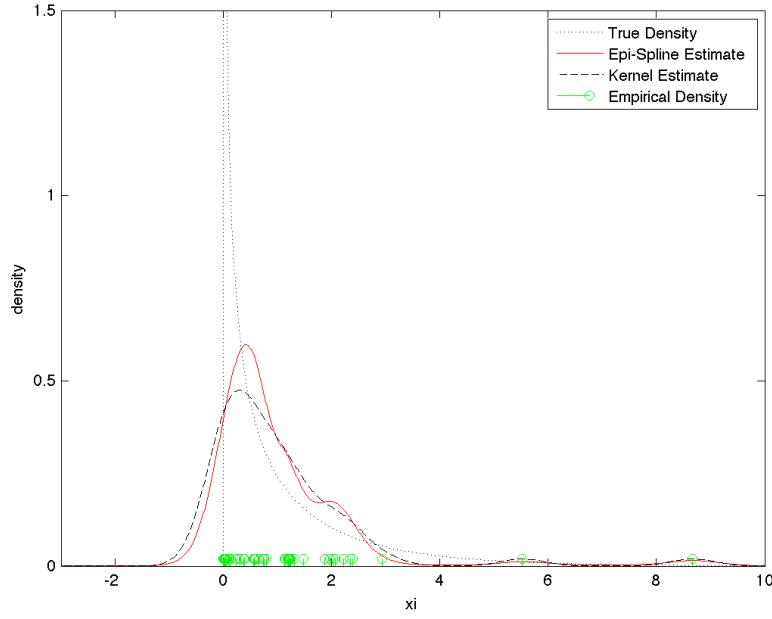
Figure 3.3: Density estimate of $\xi = G(\omega) = \omega^2$ with no soft information and $n = 50$.

Table 3.1 shows the MSEs of the fits depicted in Figures 3.2 - 3.5. Note that the MSE tends to decrease as we would expect as the sample size increases. The clear exception in this case is

17
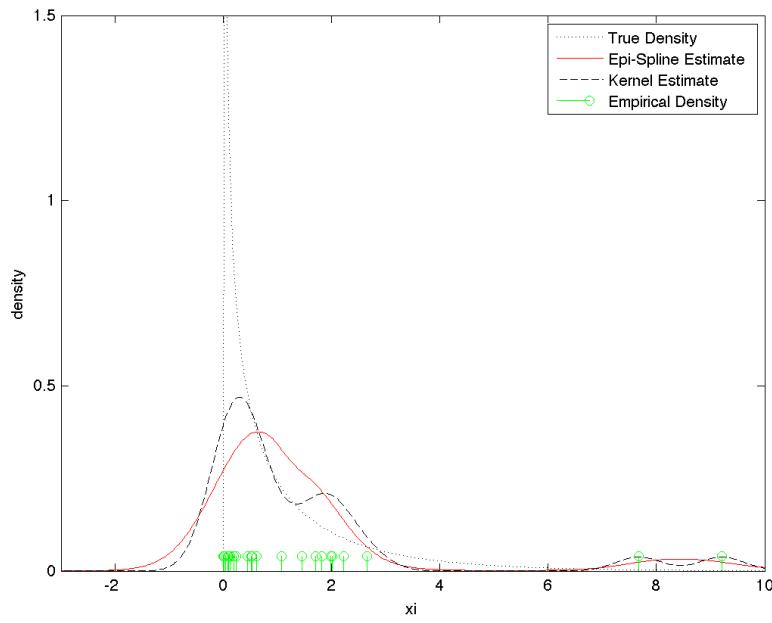
Figure 3.4: Density estimate of $\xi = G(\omega) = \omega^2$ with no soft information and $n = 25$.
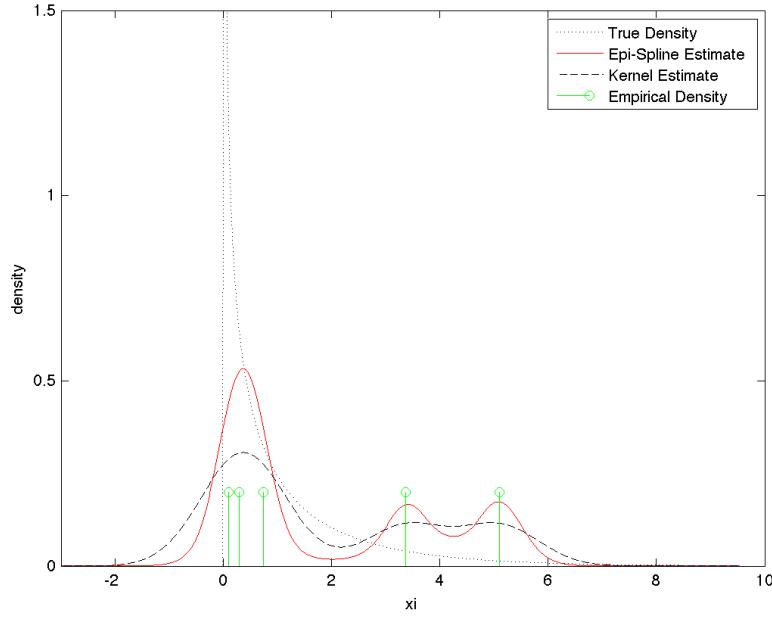

Figure 3.5: Density estimate of $\xi = G(\omega) = \omega^2$ with no soft information and $n = 5$.

with $n = 50$. This highlights a key point to make early in the presentation of our analysis. The data sets being used are being generated randomly using Matlab's random number generator. As

such, any single data set generated can vary significantly from another until a reasonable level of asymptotic behavior is reached. For the data set sizes we are considering, even at $n = 100$, we are not at the point where consistent asymptotic behaviors will be seen. So what we see in this particular case with $n = 50$ is a sample that does not fit into the expected pattern because it is a single sample set that happens to have some unique characteristics. Later, we examine average MSE of various cases to analyze a more statistically significant result than a single case comparison.

Table 3.1: MSE statistics of $\xi = G(\omega) = \omega^2$ with no soft information.

	Sample Size			
	100	50	25	5
Kernel Estimate	0.315614	0.441801	0.344619	1.018454
Epi-Spline Estimate	0.331898	0.424908	0.405645	0.936841

An interesting result, however, from Table 3.1 is that while the kernel estimate performs better at $n = 100, 50, 25$, the epi-spline performed better with the least amount of data with $n = 5$. To confirm this result in a more rigorous manner, we generate fifty random data sets of five points from the prescribed function G and estimate densities for each of the fifty replications. We perform this testing with samples of five since we are primarily concerned with performance in small data set situations, and because this is a difficult condition to obtain good estimates. The results for the kernel and epi-spline estimates are shown in Table 3.2. The results are encouraging. With an average MSE of almost half that of the kernel estimate and a 96% reduction in standard deviation, the epi-spline estimate performs well with very limited information.

Table 3.2: MSE statistics from 50 replications of $\xi = G(\omega) = \omega^2$ with $n = 5$ and no soft information.

	Average	Standard Deviation
Kernel Estimate	1.432893	2.394339
Epi-Spline Estimate	0.749545	0.086183

We now explore the addition of various aspects and levels of soft information. First, we show the impact of the various types of available soft information individually and then we show their impact when applied in concert with one another. We use the same randomly generated data

sets used in the *no soft information* case throughout in order to make valid comparisons between them. Figures 3.6 - 3.9 show the impact with the unimodality constraint implemented.
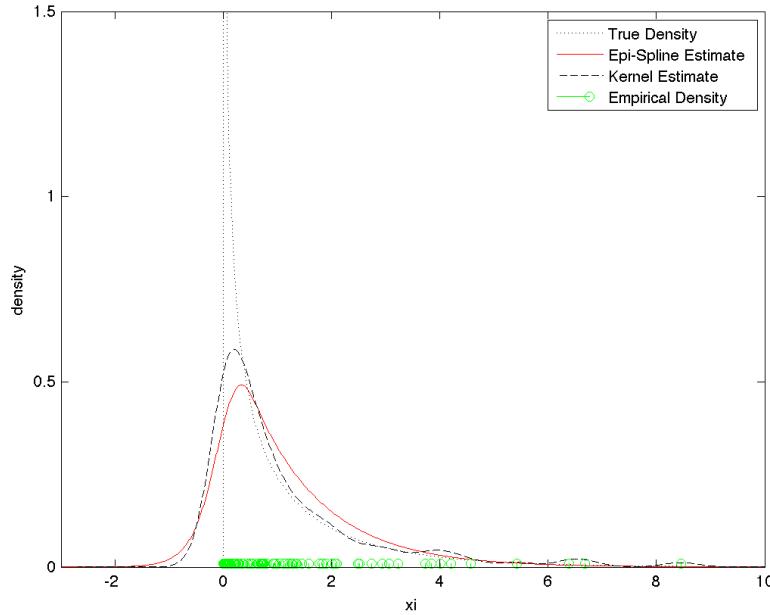

Figure 3.6: Density estimate of $\xi = G(\omega) = \omega^2$ with unimodal constraint and $n = 100$.

Table 3.3: MSE of $\xi = G(\omega) = \omega^2$ with unimodal constraint.

	Sample Size			
	100	50	25	5
Kernel Estimate	0.315614	0.441801	0.344619	1.018454
Epi-Spline Estimate	0.350229	0.432829	0.429347	1.024610

The soft information constraint forces a unimodal density function as desired; however, from visual inspection, the fit does not seem to improve all that much. The *noise* in the estimates created from outlier points is smoothed with the unimodal constraint, but overall it does not improve the fit in relation to the true density. Table 3.3 confirms this result in terms of MSE. Although the epi-spline and kernel estimates are still quite similar at $n = 100$, the epi-spline fit based on MSE has worsened from the no information case.
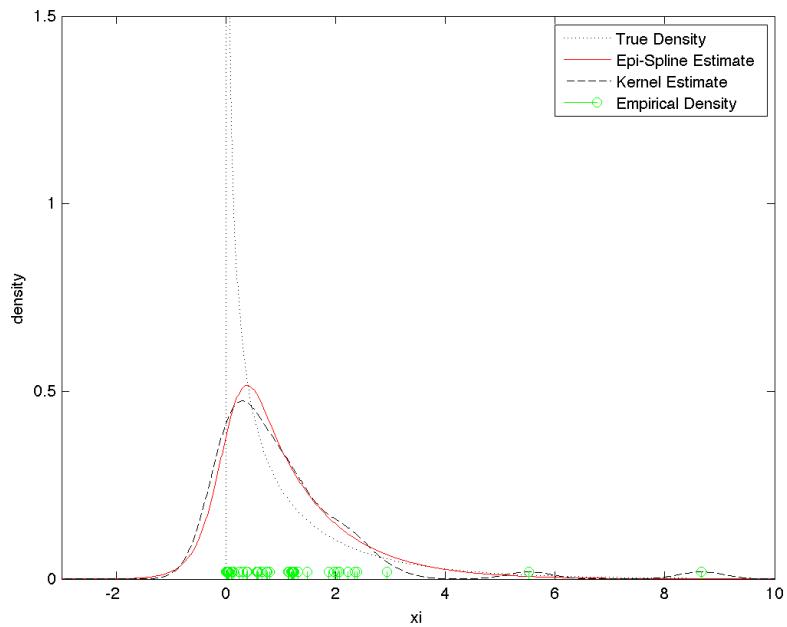
Figure 3.7: Density estimate of $\xi = G(\omega) = \omega^2$ with unimodal constraint and $n = 50$.
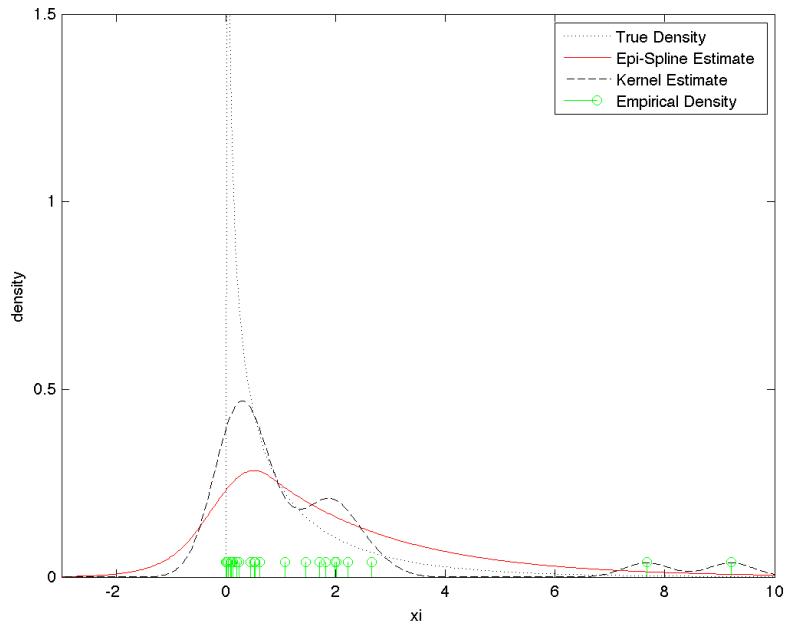
Figure 3.8: Density estimate of $\xi = G(\omega) = \omega^2$ with unimodal constraint and $n = 25$.
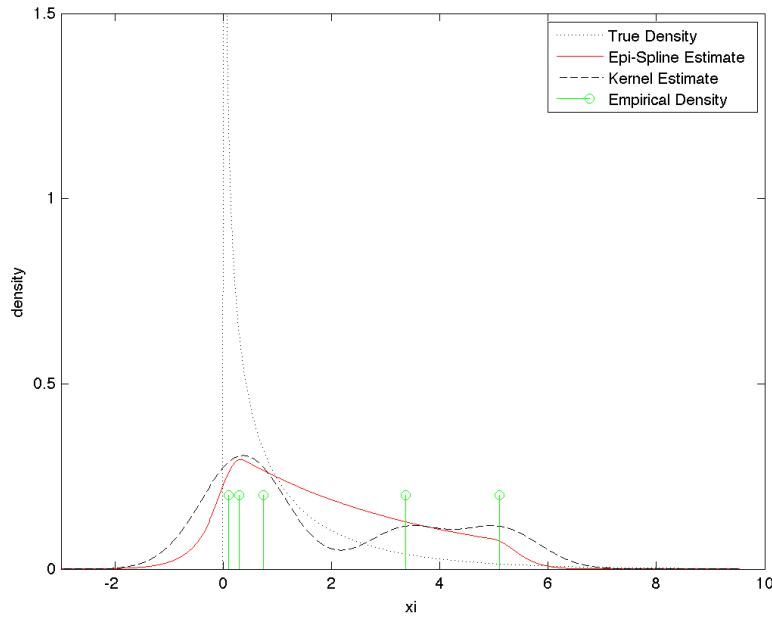
Figure 3.9: Density estimate of $\xi = G(\omega) = \omega^2$ with unimodal constraint and $n = 5$.

In stark contrast, the estimates with only a non-negative support bound implemented produce much better fits based on visual inspection. Figures 3.10 - 3.13 illustrate these results.

Table 3.4: MSE of $\xi = G(\omega) = \omega^2$ with non-negative support.

	Sample Size			
	100	50	25	5
Kernel Estimate	0.016502	0.014951	0.008257	0.032190
Epi-Spline Estimate	0.018888	0.019785	0.017624	0.157543

Table 3.4 shows the MSEs of the estimates based on non-negative support only. Note that the MSEs for the kernel estimates are different than the previous kernel estimates for these same data sets. Matlab allows for the inclusion of support information in its kernel based density estimates. In order to make a more accurate and objective comparison of the performance between the two estimation methods, we include the support information available in both.
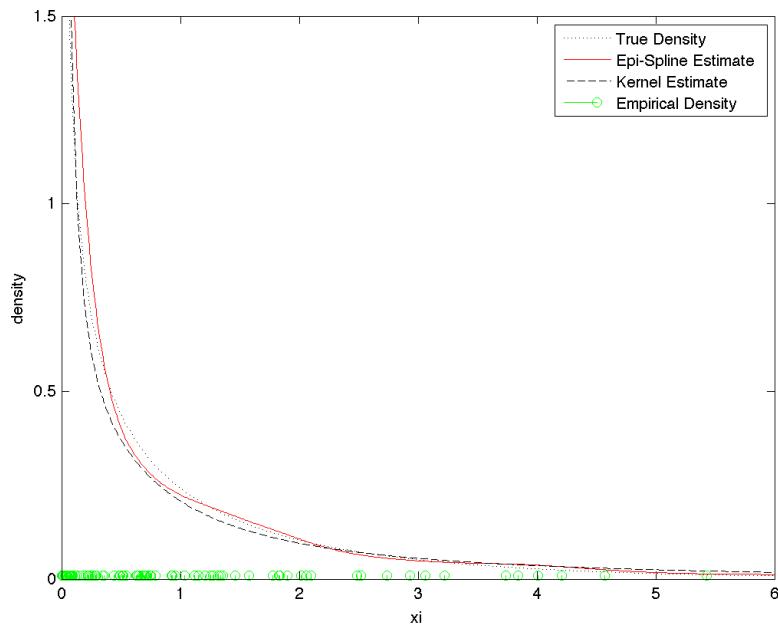
Figure 3.10: Density estimate of $\xi = G(\omega) = \omega^2$ with non-negative support and $n = 100$.
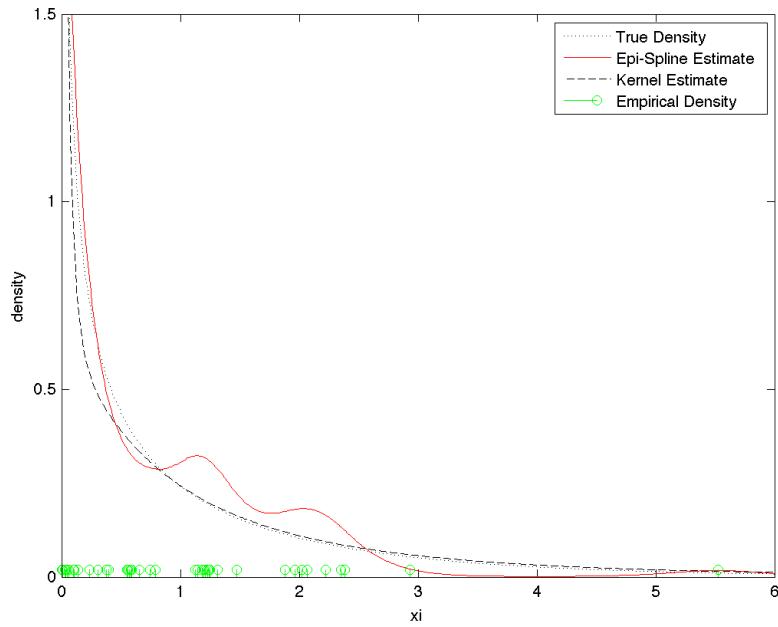

Figure 3.11: Density estimate of $\xi = G(\omega) = \omega^2$ with non-negative support and $n = 50$.
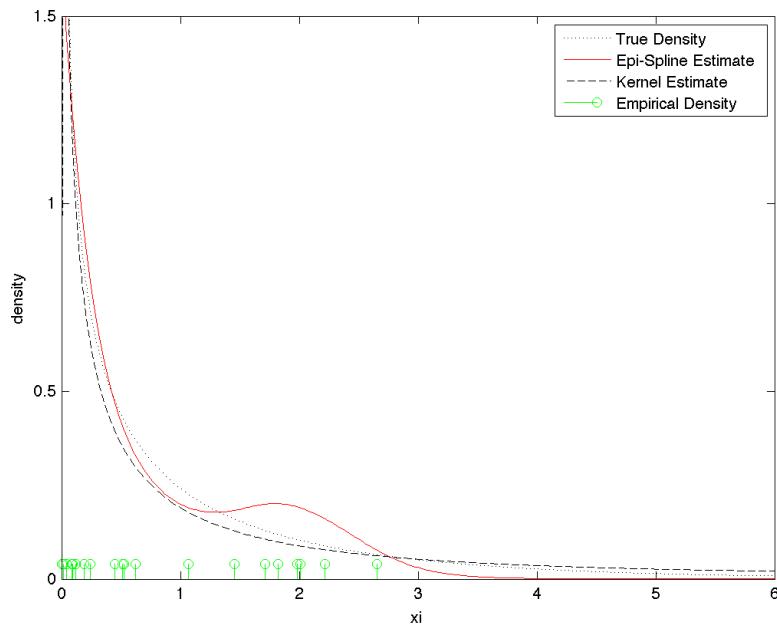
Figure 3.12: Density estimate of $\xi = G(\omega) = \omega^2$ with non-negative support and $n = 25$.
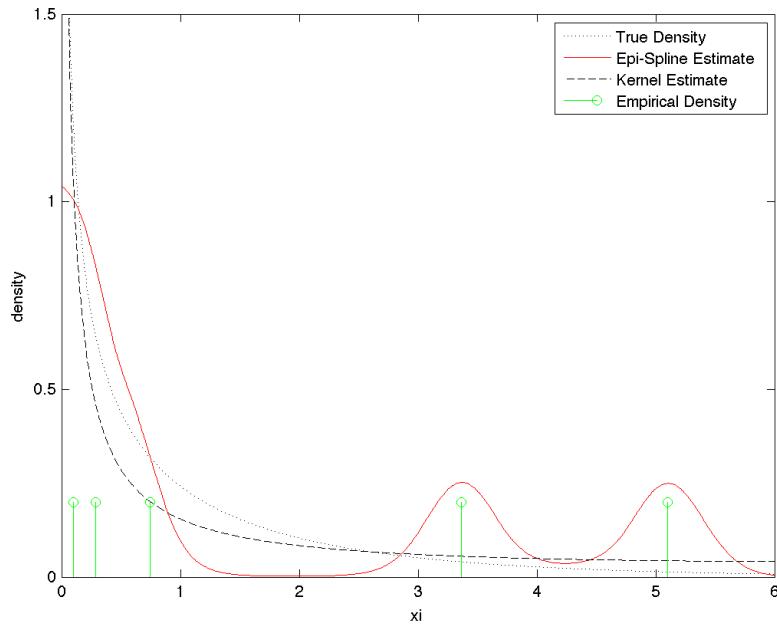
Figure 3.13: Density estimate of $\xi = G(\omega) = \omega^2$ with non-negative support and $n = 5$.

3.1.2 High Information Case

We now consider the high information case in which all of the soft information considered up to this point is combined in a single estimate. Table 3.5 and Figures 3.14-3.17 show the results when non-negative support is combined with the decreasing function constraint. Note that we do not need to explicitly include the unimodal constraint. Unimodality is implicit in a decreasing function so we can enforce both aspects of the shape with a single constraint. We also note that the kernel estimate MSE remains the same as in the case of non-negative support only. The kernel estimate is only able to incorporate support information, so it does not change with the additional information introduced here.

Table 3.5: MSE of $\xi = G(\omega) = \omega^2$ with non-negative support and decreasing constraint.

	Sample Size			
	100	50	25	5
Kernel Estimate	0.016502	0.014951	0.008257	0.032190
Epi-Spline Estimate	0.104203	0.096221	0.140380	0.271249
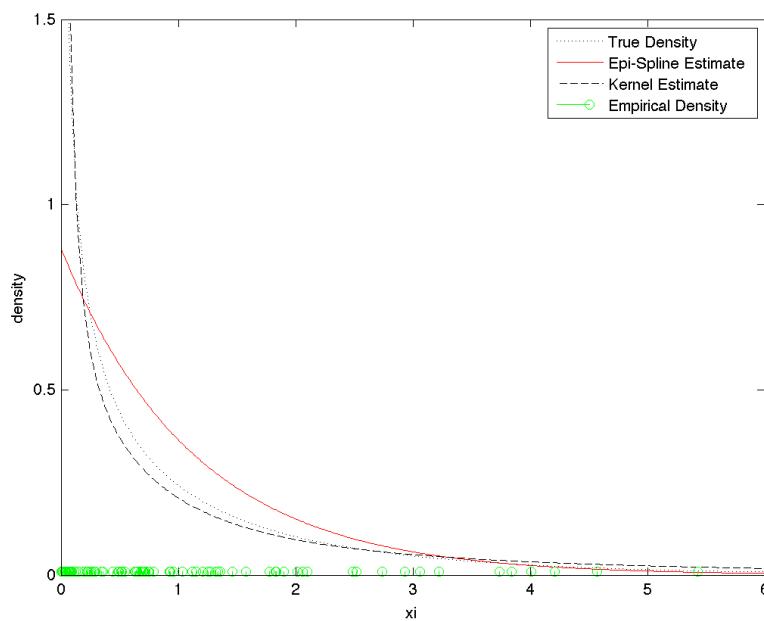
Figure 3.14: Density estimate of $\xi = G(\omega) = \omega^2$ with non-negative support, decreasing constraint, and $n = 100$.

25
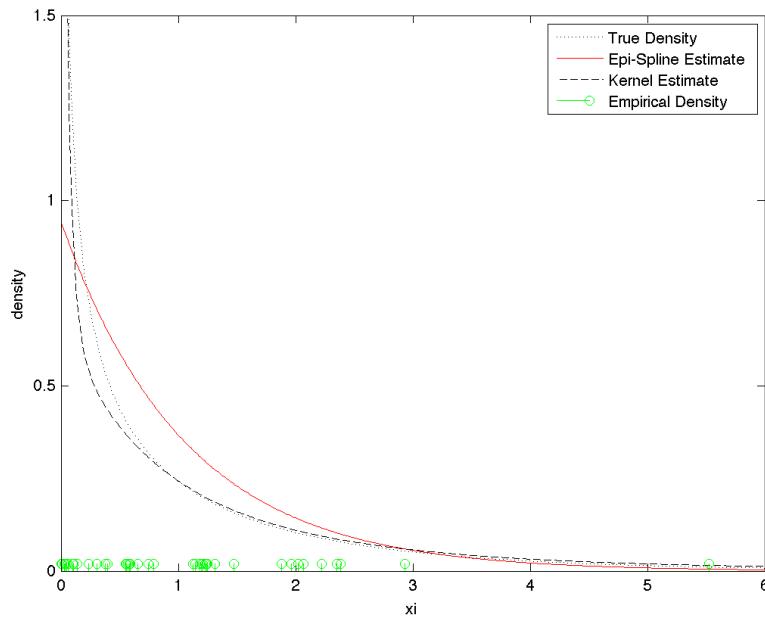
Figure 3.15: Density estimate of $\xi = G(\omega) = \omega^2$ with non-negative support, decreasing constraint, and $n = 50$.
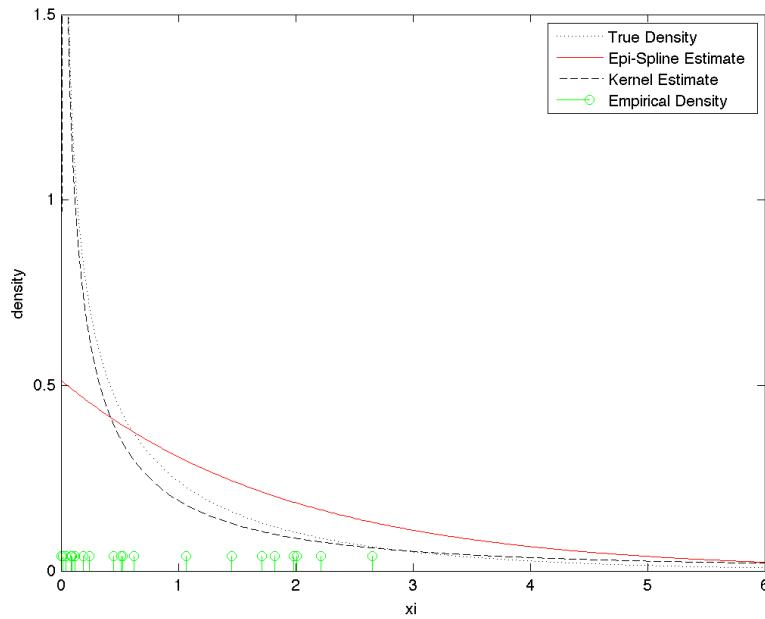

Figure 3.16: Density estimate of $\xi = G(\omega) = \omega^2$ with non-negative support, decreasing constraint, and $n = 25$.

26
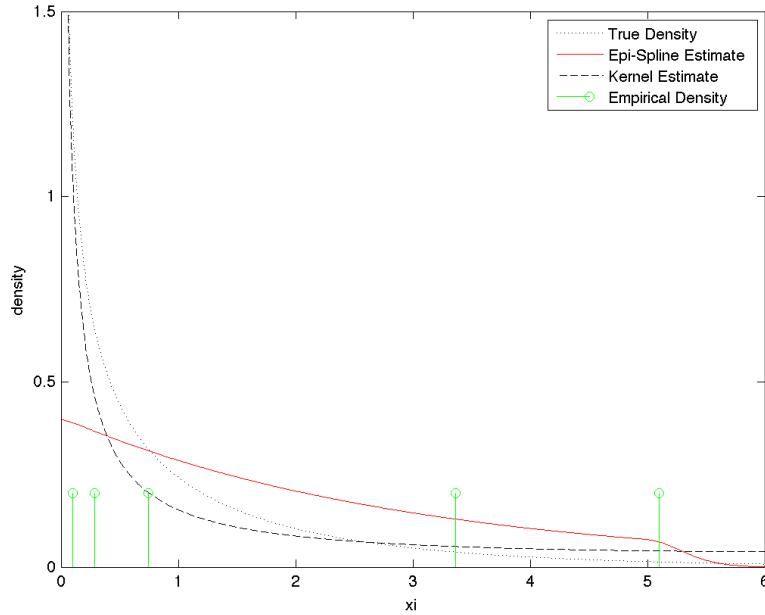
Figure 3.17: Density estimate of $\xi = G(\omega) = \omega^2$ with non-negative support, decreasing constraint, and $n = 5$.

For a more rigorous analysis of the performance comparison between the kernel estimate and the epi-spline estimate, we again perform fifty replications of the test scenario. Table 3.6 shows that, although we saw higher MSE levels with the epi-spline estimates in the anecdotal data case above, the epi-spline estimate performs well in comparison to the kernel estimate. The average MSE of the epi-spline estimate in the case of no soft information was 0.749545. With the addition of basic soft information, we see a 75% reduction in the average MSE and with a very similar standard deviation.

Table 3.6: MSE statistics from 50 replications of $\xi = G(\omega) = \omega^2$ with non-negative support, decreasing constraint, and $n = 5$.

	Average	Standard Deviation
Kernel Estimate	5.912541	20.029658
Epi-Spline Estimate	0.187737	0.071299

The small standard deviations that we see in the epi-spline estimates are of particular note. The fact that the estimates perform this well with only five data points speaks strongly of its potential for practical application. In addition, the wide ranging performance of the kernel estimate in the context of small data sets indicates that, at a minimum, great care must be used when applying a kernel based estimation process to a small data problem situation.

Now we consider a variation of the quadratic case to illustrate the application of soft information related to the Kullback-Leibler (KL) divergence discussed in Chapter 2. The idea behind applying this as soft information is that there is some qualitative knowledge about what the shape of the output density should be like. Maybe this comes from a subject matter expert familiar with the system. By applying bounds on the KL divergence measure we are able to restrict the distance of the estimate from a known density. The tighter the bound on the divergence, the more the estimate will mirror the known *reference* density. Recall the notation $d_{KL}(h||e^{-s(\cdot)}) \leq c$ to mean that the KL divergence measure between the known *reference* density h and the epi-spline estimate $e^{-s(\cdot)}$ must be within some stipulated constant c.

For this test case, consider the sum of the squares of ten standard normal random variables, i.e., $\xi = G(\omega) = \omega_1^2 + \omega_2^2 + \cdots + \omega_{10}^2$ where $\omega_i \sim N(0,1)$. This construction creates a true density $h(\xi)$ which is chi-square with ten degrees of freedom, $X^2(10)$. Figure 3.18 shows the results of the estimates based on five data points and no soft information.
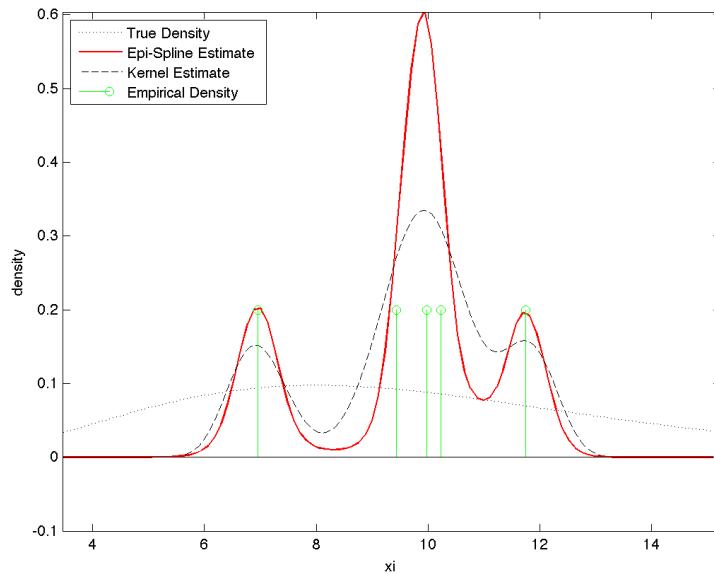
Figure 3.18: Density estimates of $\xi = G(\omega) = \omega_1^2 + \cdots + \omega_{10}^2$ with $n = 5$.

First, we include the basic soft information that is available – non-negative support and uni-modal shape. This result is shown in Figure 3.19.
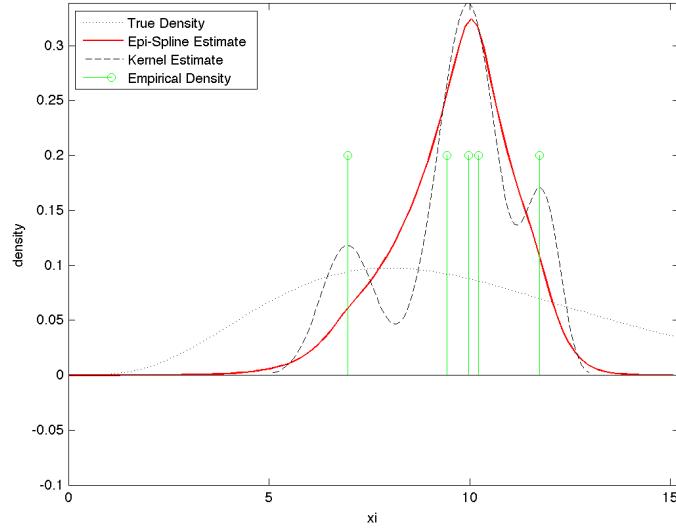
Figure 3.19: Density estimates of $\xi = G(\omega) = \omega_1^2 + \cdots + \omega_{10}^2$ with non-negative support, uni-modal, and $n = 5$.

We then add a relaxed KL divergence bound of one, shown in Figure 3.20.
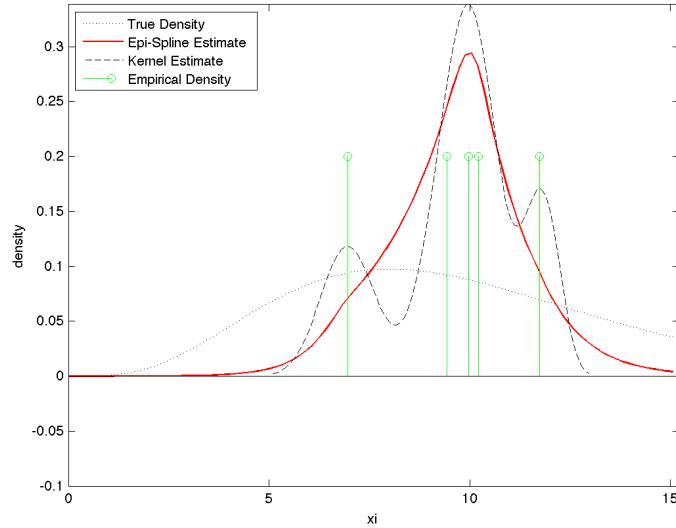
Figure 3.20: Density estimates of $\xi = G(\omega) = \omega_1^2 + \cdots + \omega_{10}^2$ with non-negative support, uni-modal, $d_{KL} \leq 1$, and $n = 5$.

The addition of the initial KL bound of one brings down the peak of the epi-spline estimate ever so slightly. We then show the impact of gradually decreasing the bound to 0.1 and then to 0.01 in Figures 3.21 and 3.22, respectively. The epi-spline fit improves significantly as the bound decreases, and at the final value of 0.01, the estimate is much closer to the general shape characteristic of the true density.
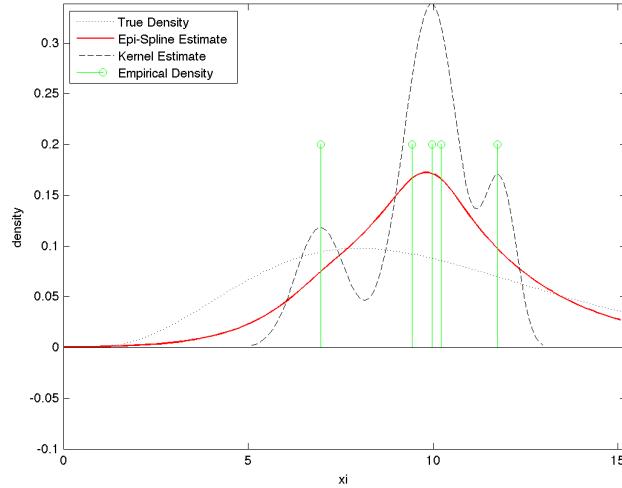
Figure 3.21: Density estimates of $\xi = G(\omega) = \omega_1^2 + \cdots + \omega_{10}^2$ with non-negative support, unimodal, $d_{KL} \leq 0.1$, and $n = 5$.
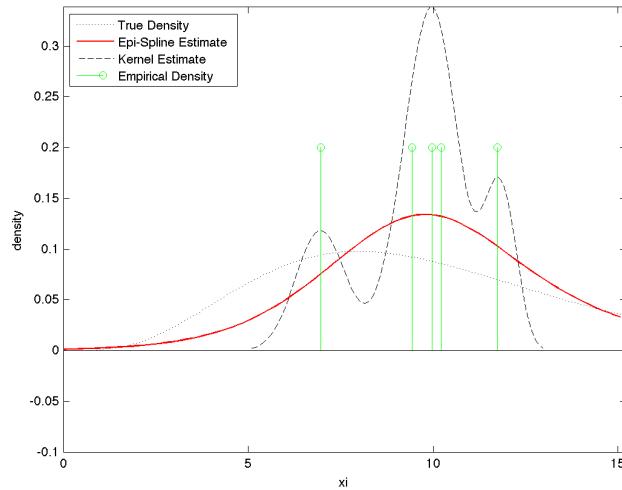

Figure 3.22: Density estimates of $\xi = G(\omega) = \omega_1^2 + \cdots + \omega_{10}^2$ with non-negative support, unimodal, $d_{KL} \leq 0.01$, and $n = 5$.

3.2 Exponential

We now consider a second analytic case where we, again, can compare results to a true known density. In this case $\xi = G(\omega) = e^{\omega}$ where $\omega \sim N(0,1)$. With this construction, we know that the density h is Log Normal with a mean of zero and variance of one, $\text{LogN}(0,1)$, see Figure 3.23. Again, we have some information about G, ω, and ξ. We know $\xi = G(\omega) = e^{\omega}$ will produce only non-negative output, so we can implement a left support bound of 0. We also know that the density is unimodal. Unlike $G(\omega) = \omega^2$, however, we do not have a decreasing function in this case. We will use this example to explore other types of soft information constraints that were discussed in Chapter 2. At this point we have shown the effect of sample size, so we restrict our illustrations to cases with smaller data sets, i.e., $n = 5$ and 25.
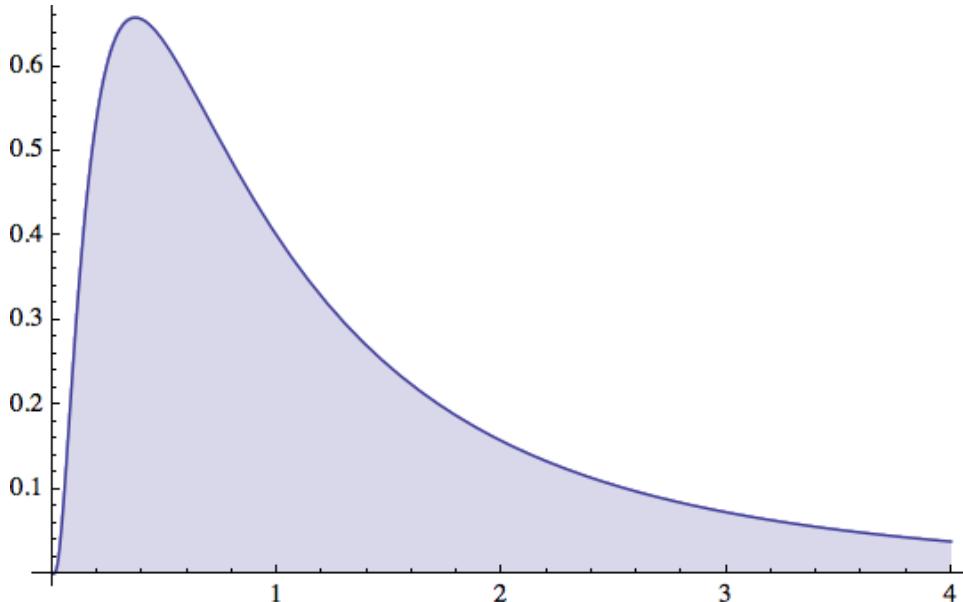
Figure 3.23: LogNormal$(0, 1)$ density.

3.2.1 Low Information Cases

First, we consider the comparison of the epi-spline estimate including no soft information versus the kernel estimate shown in Figures 3.24 and 3.25. We see clearly that the epi-spline estimate based on five observations is a bit noisy without any additional information.

Both the kernel and epi-spline estimates improve dramatically with 25 observations; however, from visual inspection the epi-spline appears to better capture the density near zero where the
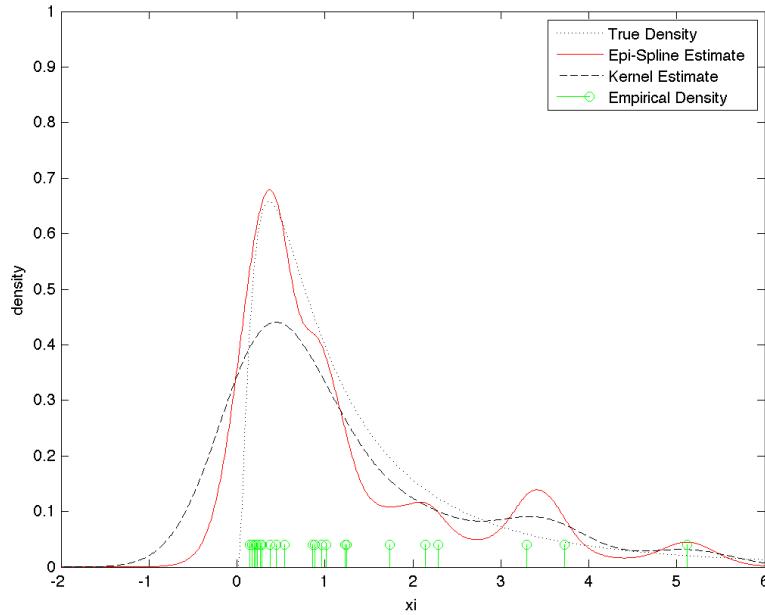
Figure 3.24: Density estimates of $\xi = G(\omega) = e^{\omega}$ with no soft information and $n = 25$.
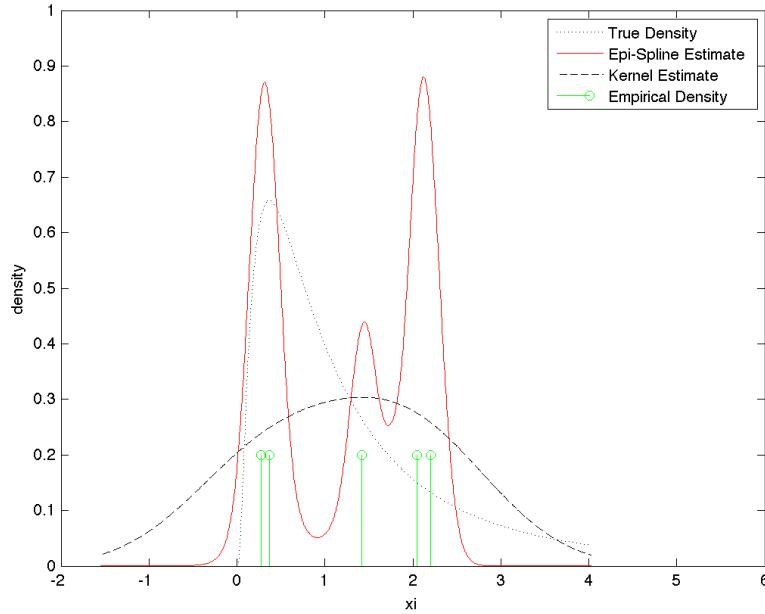
Figure 3.25: Density estimates of $\xi = G(\omega) = e^{\omega}$ with no soft information and $n = 5$.

true density peaks. This is confirmed by the MSE results in Table 3.7, which summarizes the MSE results for the three low information cases we present.

Table 3.7: MSE for low information cases of $\xi = G(\omega) = e^{\omega}$.

	$n = 25$	$n = 5$
Kernel Estimate	0.066753	0.119479
Kernel - non-negative support	0.167938	0.065961
Epi-Spline - no soft information	0.039013	0.265073
Epi-Spline - unimodal	0.026743	0.114233
Epi-Spline - unimodal, non-negative support	0.026871	0.116977

Unlike the previous example of $G(\omega) = \omega^2$, the MSE for the epi-spline estimate with no soft information for the random data set is worse than the kernel estimate. To better determine its true performance, we conduct fifty replications of the estimates on random data sets of size five. Table 3.8 shows that, once again, the epi-spline estimate performs significantly better than the kernel estimate in a very limited data context, particularly in terms of its variability.

Table 3.8: MSE statistics from 50 replications of $\xi = G(\omega) = e^{\omega}$ estimates with no soft information and $n = 5$.

	Average	Standard Deviation
Kernel Estimate	0.526273	2.215139
Epi-Spline Estimate	0.403309	0.269902

With the unimodal constraint included in the estimation, the epi-spline estimates for both sample sizes shown in Figures 3.26 and 3.27 improve dramatically. And while the estimate with $n = 5$ may visually look a bit strange, the MSE of the estimate is less than that of the kernel estimate. For relatively little information, the epi-spline estimate with $n = 25$ is surprisingly accurate.

In this particular example, the addition of the support bound constraint restricting the density to non-negative values does not improve the overall estimate. These fits are shown in Figures 3.28 and 3.29. The change in MSE from the unimodal constraint only is insignificant and the overall shape of the density is not dramatically changed.

3.2.2 High Information Cases

For the high information cases, we consider several interesting soft information implementations which have not yet been illustrated in this thesis. We analyze the impact of including
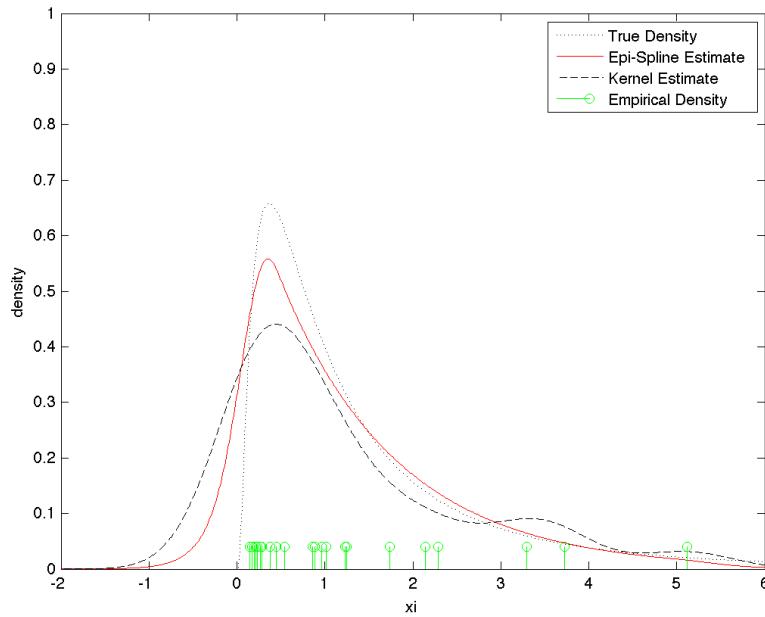
Figure 3.26: Density estimates of $\xi = G(\omega) = e^{\omega}$ with unimodal constraint and $n = 25$.
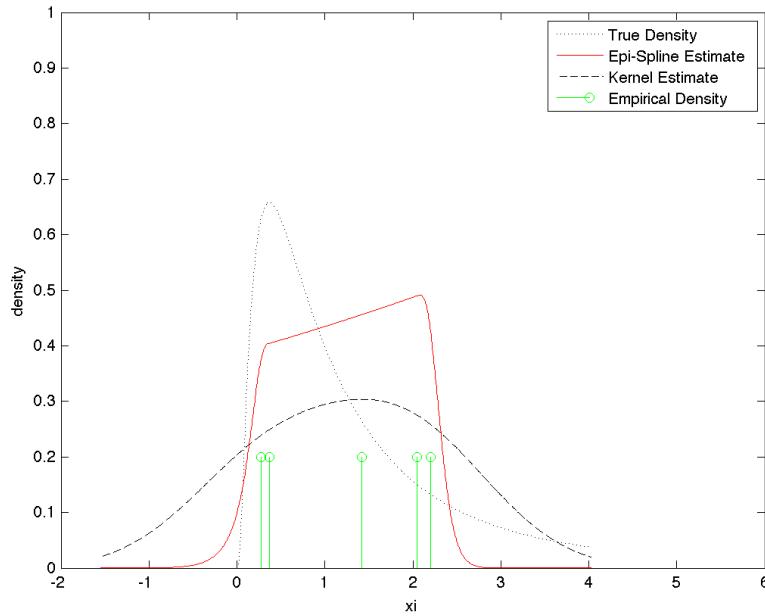
Figure 3.27: Density estimates of $\xi = G(\omega) = e^{\omega}$ with unimodal constraint and $n = 5$.

gradient information and bounds on the value of the epi-spline at the initial point in the support of the estimate, d_0.
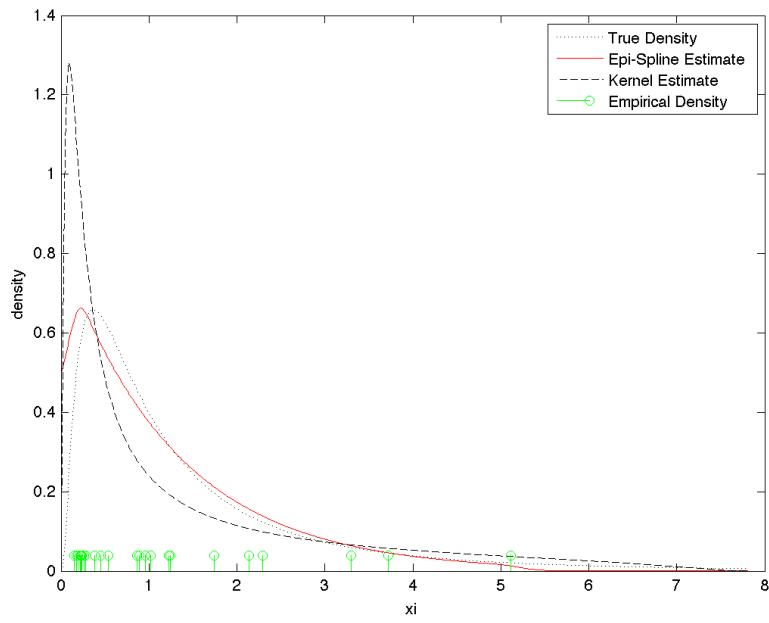
Figure 3.28: Density estimates of $\xi = G(\omega) = e^\omega$ with unimodal constraint, non-negative support, and $n = 25$.
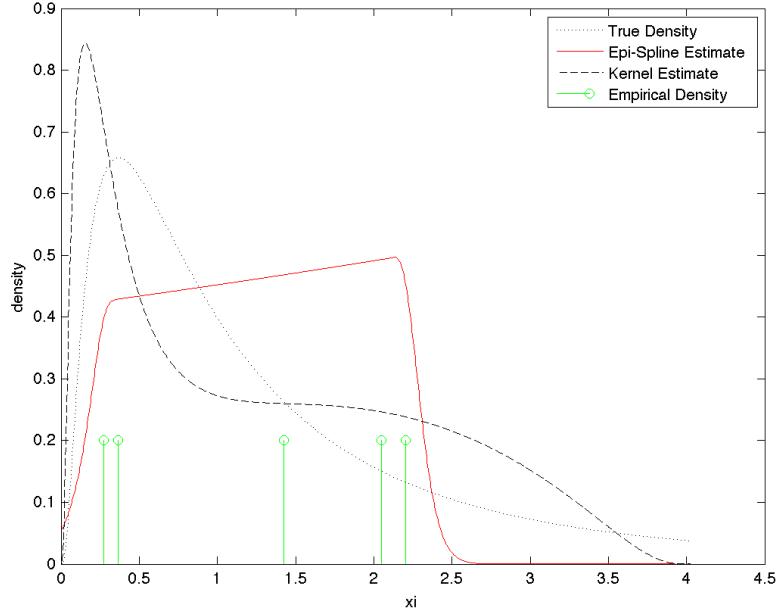
Figure 3.29: Density estimates of $\xi = G(\omega) = e^\omega$ with unimodal constraint, non-negative support, and $n = 5$.

Suppose a situation where, although *G* may be unknown in terms of being able to explicitly formulate a mathematical expression that accurately reflects the system in question, gradient information related to particular system output values is known. While this may initially sound like a highly manufactured situation for illustrating this source of soft information, this is a realistic scenario. Extracting gradient information from complex systems such as large scale simulations is an area of research all its own. There continues to be extensive research in this area and there are currently several methods for precisely this need [13].

The motivation behind these techniques for extracting the gradient information is actually somewhat similar to the motivation for this research. In situations where the simulation is so costly in terms of time and/or money, conducting a large number of replications may be impractical. The need to do sensitivity analysis on the system performance motivates the application of these gradient extraction techniques.

Figures 3.30 and 3.31 show the impact of gradient information at one data point. Although the shape of the epi-spline estimate does not change significantly, in the $n = 5$ case the MSE decreases substantially, see Table 3.9.
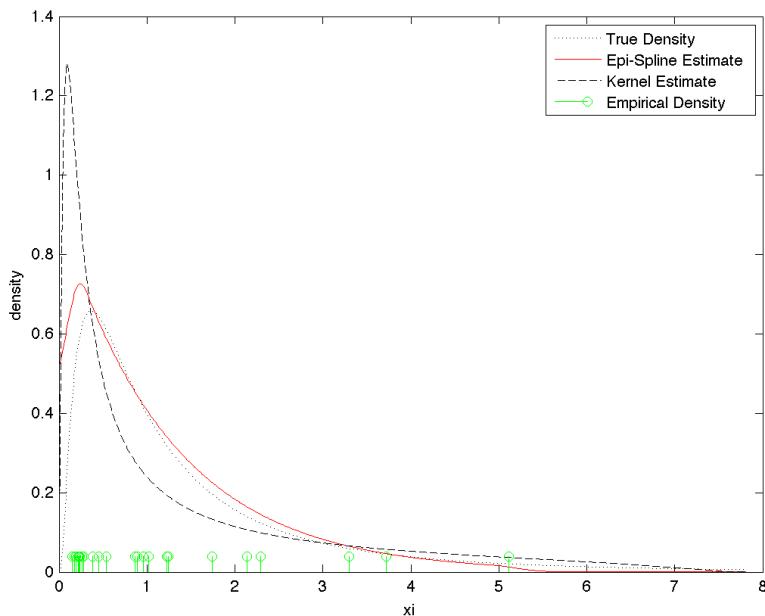
Figure 3.30: Density estimates of $\xi = G(\omega) = e^{\omega}$ with unimodal constraint, non-negative support, gradient at 1 point, and $n = 25$.

In the $n = 25$ case, Figure 3.30, the fit is already quite good for the particular sample so the addition of gradient information at one point does not improve the estimate. However, for a comparable percentage of gradient information points from the overall sample size, i.e., one point out of five is 20%, we consider five gradient points in the $n = 25$ case.
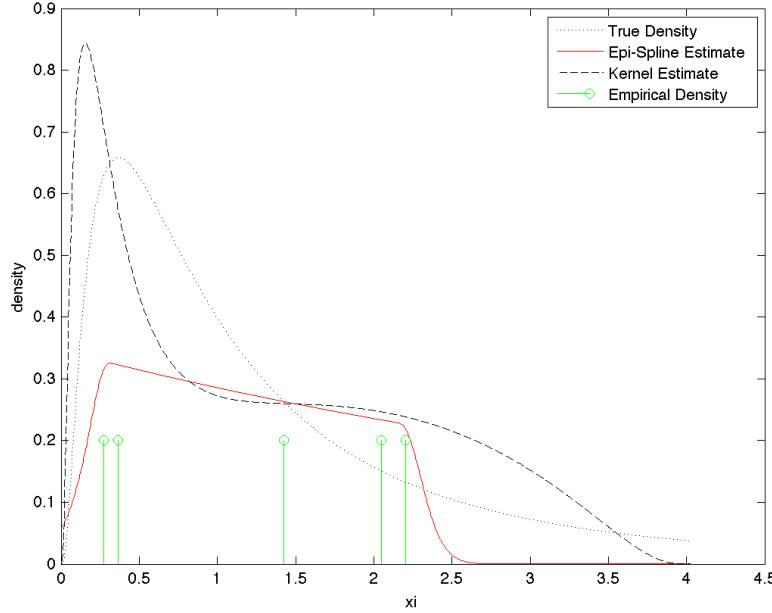

Figure 3.31: Density estimates of $\xi = G(\omega) = e^{\omega}$ with unimodal constraint, non-negative support, gradient at 1 point, and $n = 5$.

Table 3.9: MSE for high information cases of $\xi = G(\omega) = e^{\omega}$.

	$n = 25$	$n = 5$
Kernel Estimate	0.167938	0.065961
Epi-Spline - gradient at 1 point	0.031002	0.075030
Epi-Spline - gradient at 5 points	0.012840	0.023152
Epi-Spline - gradient at 5 points, bounds on d_0	0.004925	0.005560

Note: all epi-spline estimates include unimodal constraint and non-negative support.

Figures 3.32 and 3.33 show the resulting estimates with gradient information at five points. Obviously, in the $n = 5$ case, this constitutes gradient information at all points so the estimate improves dramatically by visual inspection and by MSE. Also, as we would expect, the estimate improves dramatically in the $n = 25$ case. The gradient information is implemented as an

equality constraint in the estimation problem, so it clearly has a strong implication in the results of the overall estimate.
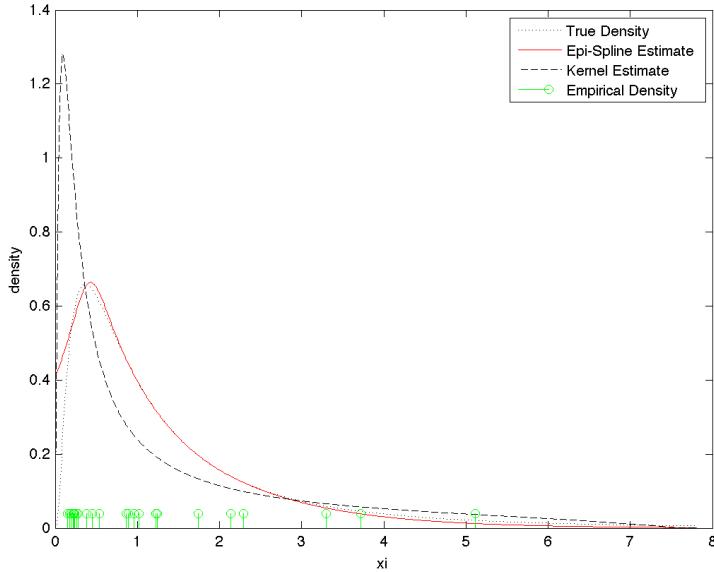
Figure 3.32: Density estimates of $\xi = G(\omega) = e^{\omega}$ with unimodal constraint, non-negative support, gradient at 5 points, and $n = 25$.
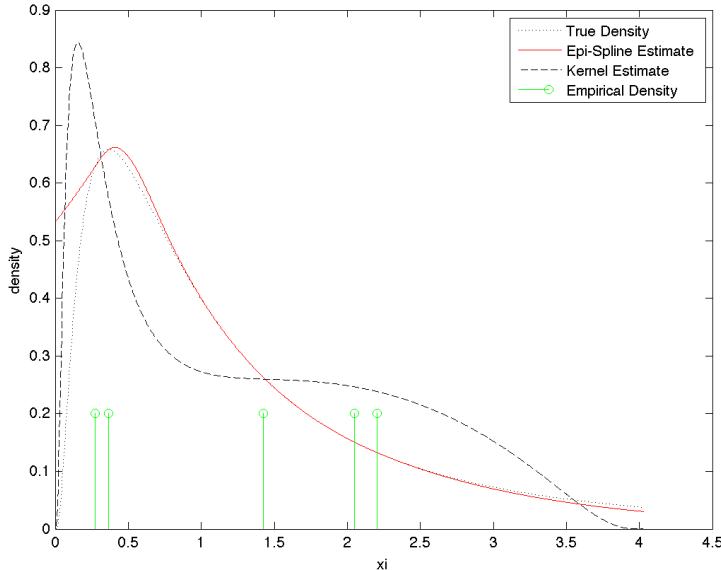
Figure 3.33: Density estimates of $\xi = G(\omega) = e^{\omega}$ with unimodal constraint, non-negative support, gradient at 5 points, and $n = 5$.

The last type of soft information we consider in this test case is regarding a bound on the value of the epi-spline at the initial point in the density support, d_0, which is very applicable in this example. We have limited the density to non-negative support, but bounding the value of the epi-spline is a different type of bound. With this we are saying that the density value itself, at the initial point d_0, is bounded by some value. In this example, the support range is not only bounded at zero, but the density value at this point is also zero. With this type of soft information, we are able to restrict the density starting point closer to what we know to be the true starting point density. Figures 3.34 and 3.35 show the addition of the d_0 bound to the previous level of information.
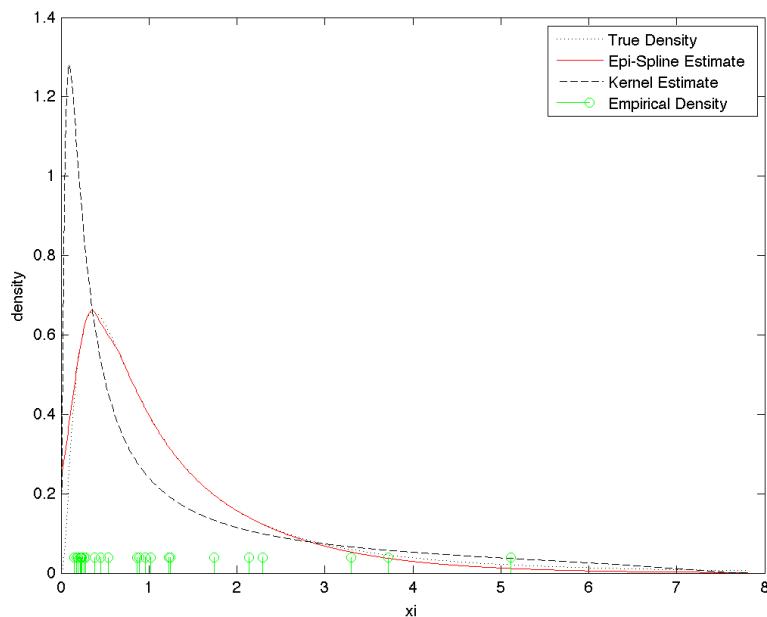

Figure 3.34: Density estimates of $\xi = G(\omega) = e^\omega$ with unimodal constraint, non-negative support, gradient at 1 point, bound on d_0, and $n = 25$.

Both sample size cases show the impact of the d_0 bound particularly well. In the $n = 25$ case, the previous estimates of the density value at d_0 were in the $0.4 - 0.5$ range. We know the true density at d_0 is in fact zero. The upper bound that was imposed in this illustration reduces the density value at d_0 to around 0.2, much closer to the actual value and significantly improving the visual fit of the estimate. In the $n = 5$ case shown in Figure 3.35, the density value at d_0 reduces to almost zero. The MSE results in Table 3.9 confirm the improvement as well. We see an order of magnitude reduction in the epi-spline MSE at both sample sizes.
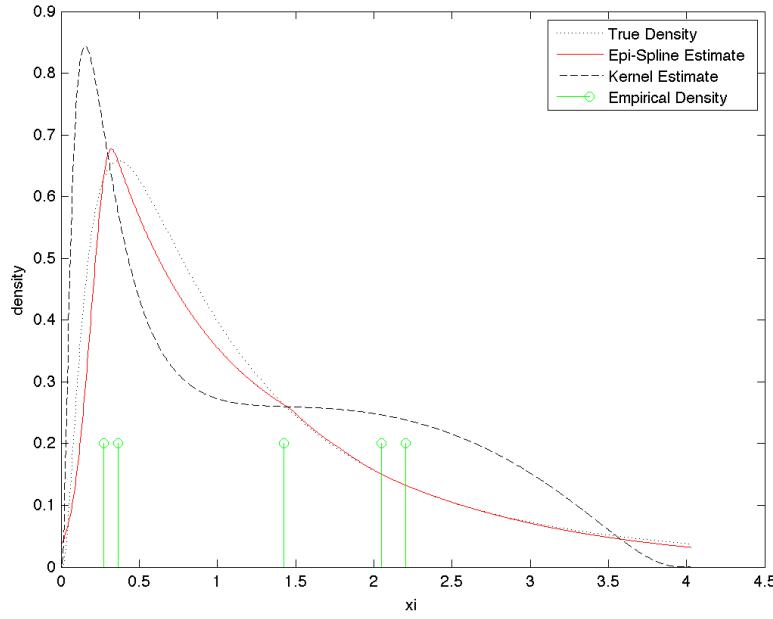
Figure 3.35: Density estimates of $\xi = G(\omega) = e^\omega$ with unimodal constraint, non-negative support, gradient at 1 point, bound on d_0, and $n = 5$.

We provide MSE statistics from fifty random replications of several high information scenarios for the exponential case with $n = 5$. Although, we see a significant improvement in the kernel statistics when the non-negative support bound is included, the epi-spline estimates continue to outperform in average MSE and its variability. The average MSE for the epi-spline with gradient information at one point is neglibly higher than the kernel estimate, but with a much larger reduction in variability the epi-spline estimates would be favored in this regard.

Table 3.10: MSE statistics from 50 replications of high information cases of $\xi = G(\omega) = e^\omega$ estimates with $n = 5$.

	Average	Standard Deviation
Kernel Estimate	0.542005	1.200533
Epi-Spline with gradient at 1 pt.	0.552342	0.998670
Epi-Spline with gradient at 2 pts.	0.277791	0.625790
Epi-Spline with gradient at 5 pts., bounds on d_0	0.232691	0.388744

Note: all epi-spline estimates include unimodal constraint and non-negative support.

3.3 Column

As a final example case, we borrow a structural engineering problem presented in UQ research done at Sandia National Laboratory [1], [5]. The problem pertains to the analysis of a rectangular column with cross section dimensions $b = 5$ and $h = 15$. We let the material have a yield stress value of $s = 5$. The column is subject to uncertain loads which bring with it two uncertain inputs to the problem – bending moment and axial force. These sources of uncertainty produce a random vector ω of length two rather than the single variable cases we have tested thus far.

Let the bending moment ω_1 be normally distributed as $N(2000, 400)$ and the axial force ω_2 be normally distributed as $N(500, 100)$ with a correlation coefficient of 0.5 between them. In this example, the system G is the column's limit-state function such that a negative value indicates failure of the column. Let

$$G(\omega) = 1 - \frac{4\omega_1}{bh^2 s} - \frac{\omega_2^2}{b^2 h^2 s^2} \tag{3.1}$$

where the random vector $\omega = (\omega_1, \omega_2)$.

There is no true density with which to make comparisons, but with full information regarding ω and a mathematical formulation for G, we are able to accurately estimate an asymptotically *true* density by taking a random sample of one million observations with a coefficient of variation of 0.0381. Figure 3.36 shows the probability density of the column mean strength based on the one million random samples.
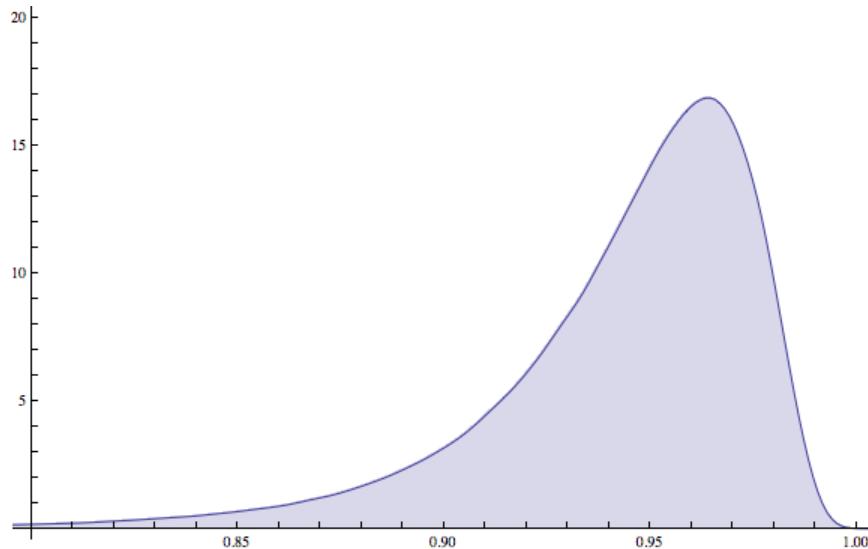
Figure 3.36: Estimated *true* density of column example based on 1 million samples.

The purpose of this example is to simply illustrate that the epi-spline estimator can effectively be applied in a more complex system scenario, as a contrast to the simple single variable examples we have shown thus far. As such, we limit this example scenario to a single data sample case for illustration purposes. We generate a random sample of $n = 20$ based on the system construction in (3.1) and explore the application of two possible sources of soft information – unimodality and gradient information. Figure 3.37 shows the epi-spline and kernel estimates with no soft information.
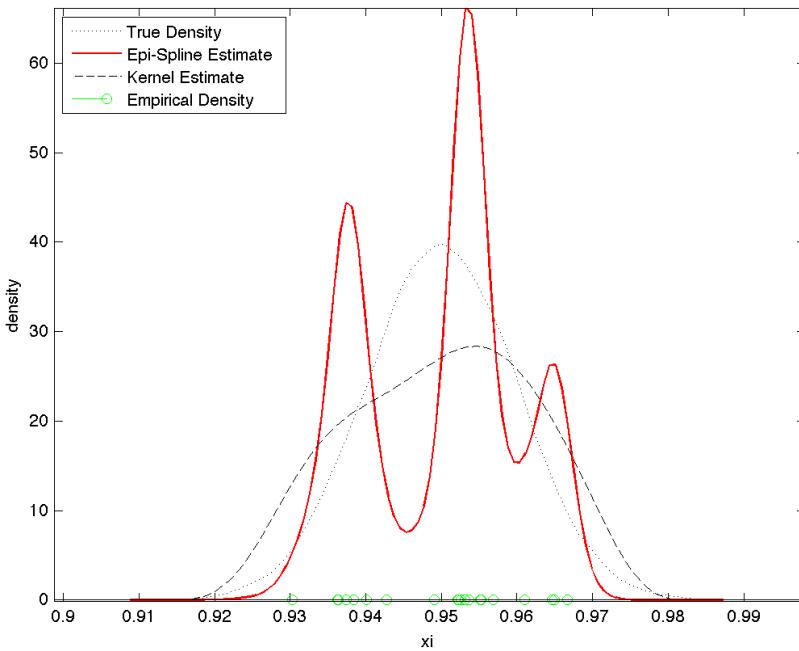
Figure 3.37: Density estimates of the column example with no soft information and $n = 20$.

With the addition of unimodality, shown in Figure 3.38, the epi-spline estimate is already quite close to the asymptotic *true* density function. Lastly, we suppose gradient information at five of the data points is available. Figure 3.39 shows that the epi-spline estimate based on the twenty data points and two information sources is almost indistinguishable from the *true* density.

This example reinforces, empirically, that the epi-spline framework may be applied successfully to more complex systems. The key is in identifying the available soft information from a particular problem context and constructing the appropriate problem constraints to enforce the desired behavior in the estimate.
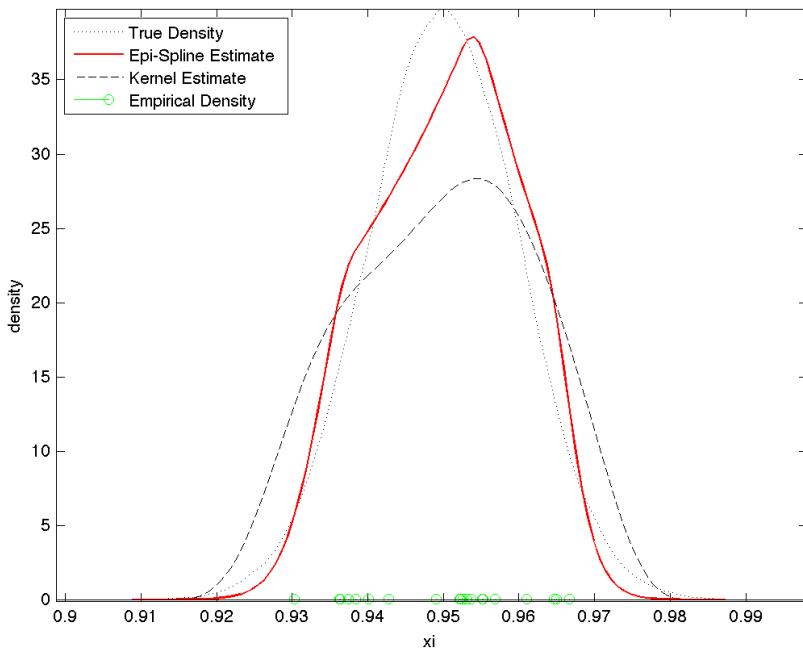
Figure 3.38: Density estimates of the column example with unimodal constraint and $n = 20$.
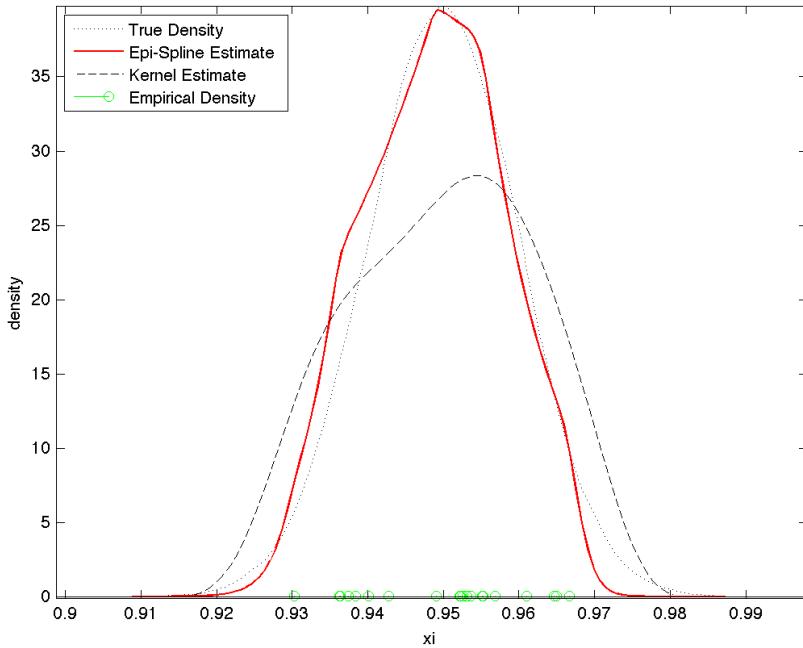
Figure 3.39: Density estimates of the column example with unimodal constraint, gradient information at 5 points, and $n = 20$.

THIS PAGE INTENTIONALLY LEFT BLANK

CHAPTER 4:
HABITABILITY ASSESSMENT TEST ANALYSIS

In this chapter, we apply the epi-spline framework to the analysis of a particular real-world problem that is the subject of another NPS thesis [14] and illustrate the potential of the framework.

4.1   Test Background and Purpose

The Habitability Assessment Test (HAT) was conducted to collect data in support of research studying the effects of waterborne motion on the combat efficiency of individual soldiers. Using personnel from the United States Marine Corps (USMC), the Amphibious Vehicle Test Branch (AVTB) conducted the HAT in August 2011 at USMC Base Camp Pendleton, California. The study defines *combat efficiency* by "functions affecting an infantryman's ability to conduct combat operations during an amphibious assault." [4] In particular, the study has focused on three primary areas of human function – physical coordination, sensory perception, and cognitive performance.

Human function is an area with a great deal of inherent uncertainty. There is, arguably, no more complex a system known to man than that of the human body. The number of variables impacting the performance of one human over another in a given setting is seemingly endless. As such, the need to quantify this uncertainty in a rigorous way for the type of research being conducted with the HAT described above is of key importance. Particularly because the results and analysis of this study, and many others like it, are informing key decisions by senior leadership within the Armed Forces.

The HAT study is of particular importance to key decisions concerning the design of future amphibious landing vehicles for the USMC. The structure of the test revolved around three basic vehicle configurations – Expeditionary Fighting Vehicle (EFV) with cooled air conditioning, EFV with vent air conditioning, and Amphibious Assault Vehicle (AAV). The test then exposed four squads of fifteen[4] to varying levels of exposure – zero hours as a control condition, one hour, two hours, and three hours – in those three different amphibious vehicle configurations.

---

[4]In the test, one of the four squads was sixteen personnel rather than fifteen, but for consistency of sample size, that squad's results have been reduced to fifteen observations for our numerical work.

Following the waterborne exposure, the Marines were then circulated through a battery of tests measuring their performance in the three human function areas previously mentioned.

We focus our analysis on the cognitive performance area of the HAT study in relation to vehicle configuration and exposure duration. We have chosen to focus on cognitive performance because results from the HAT study [4] indicate that there was an impact on cognitive throughput in relation to exposure duration. Results also stated that significant impacts to markmanship scores, a measure of sensory perception, and physical coordination performance were not observed. Specifically, we consider the percentage difference in cognitive throughput[5] following the waterborne exposure, which is used as a measure of cognitive performance.

4.2   Application of Epi-Spline Framework

In our epi-spline framework notation, the random vector ω in this case represents the various conditions of the test scenario. For example, ω is comprised of the vehicle configuration, duration of waterborne exposure, speed of the vehicle, and sea state conditions during the exposure period. The system can be thought of as the test itself, which is measuring human performance. In this case, the many human parameters of the individual Marines such as height, weight, physical condition, intelligence, etc. become part of the random vector ω and follow some probability distribution as we have seen in the Chapter 3 examples.

We desire an estimate of the density h of ξ equal to the percentage change in cognitive throughput from before the waterborne exposure to after waterborne exposure. Since we are examining the change in the cognitive measure, a negative value indicates a decrease in cognitive performance whereas a positive value indicates an increase in performance. Zero indicates no change and is interpreted as meaning that the waterborne exposure has no impact on cognitive performance.

The analysis of the data from the three vehicle configurations is a similar process, so we use the EFV - cooled air configuration as the primary illustration case. Each of the estimates is constructed from the fifteen squad member observations, so $n = 15$ in all of the estimates.

Figure 4.1 shows the density estimations for each of the four durations – 0, 1, 2, and 3 hours – under the EFV - cooled air configuration with no soft information. The noisy estimates reflect the little information available in the small data samples.

---

[5]Cognitive throughput is a measure of the number of questions answered correctly per minute on a cognitive test used in the HAT.
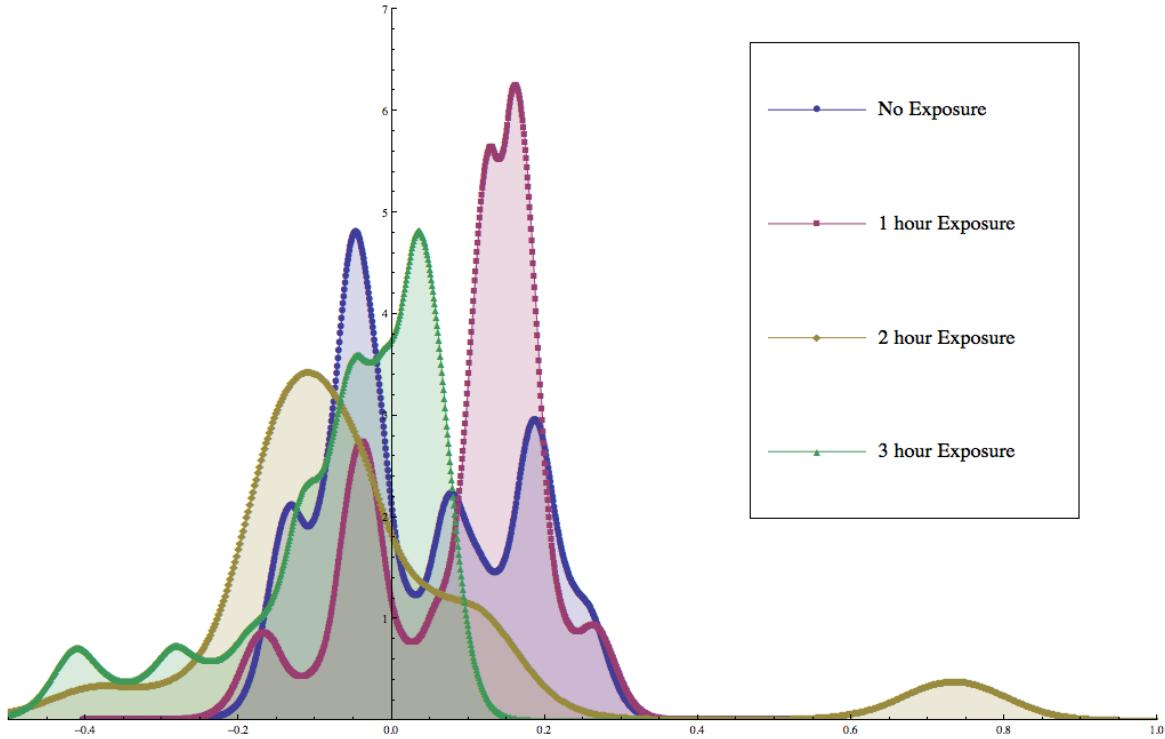
Figure 4.1: Density estimates of change in cognitive throughput based on waterborne exposure in EFV - cooled air configuration with no soft information.

We incorporate a unimodal constraint based on information from researchers familiar with the test. Initially, we hypothesized that the impact of waterborne exposure would be a degradation in performance across all of the study participants. This would have led to additional soft information concerning the densities. We anticipated the inclusion of a support bound that would prevent values that indicate an improvement in performance as a result of exposure and a monotonic constraint.

The test results, however, just do not support that hypothesis. In human factor testing, there are often confounding factors that impact results and complicate analysis. In this case, there are test observations which indicate an improvement in performance following exposure. To implement a support bound in this case is akin to discounting valid observations, which would not only decrease already small samples, but would also call into question any conclusions made from the analysis.

The estimates including the unimodal constraint are shown in Figure 4.2. Compared to the no soft information estimates, these estimates are more in line with a qualitative understanding

of the results. Specifically, consider the similarity between the one and three hour exposure estimates. Their shape is almost identical and their relationship is what we expect to see. That is, the three hour estimate is shifted to the left of the one hour estimate, which indicates that there is a greater decrease in cognitive performance with the increased exposure time.
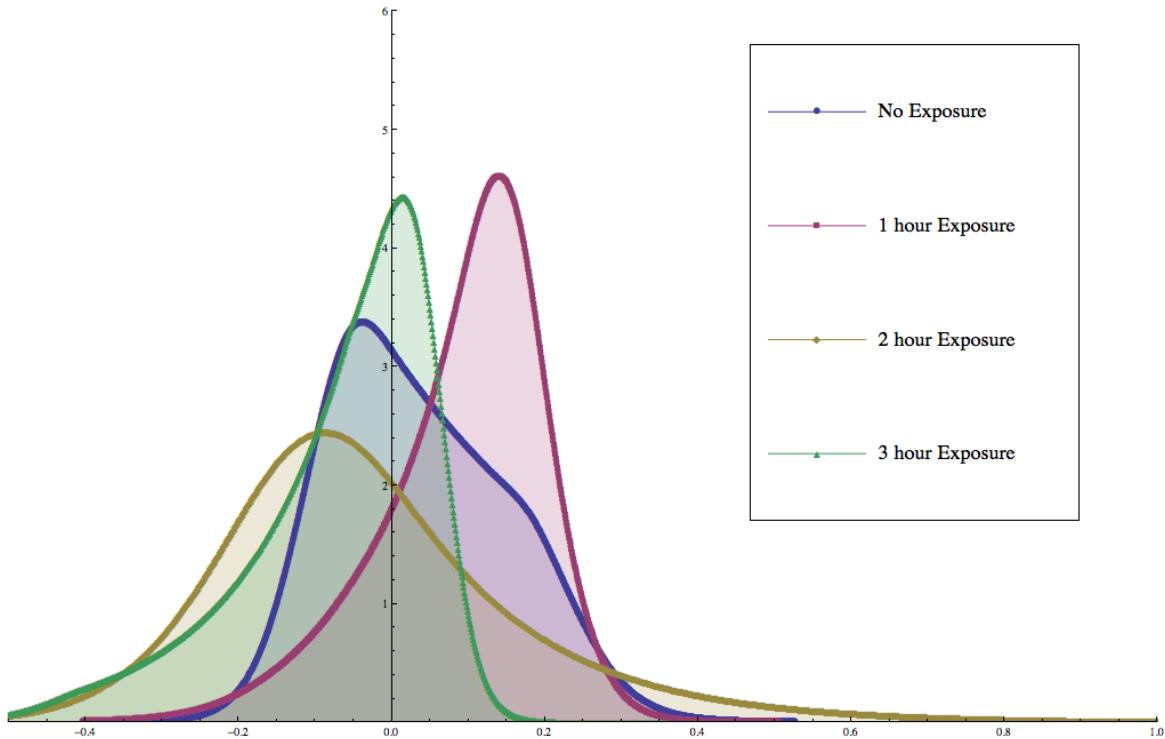

Figure 4.2: Density estimates of change in cognitive throughput based on waterborne exposure in EFV - cooled air configuration with a unimodal constraint.

This application presents some very interesting possibilities of how to leverage the flexibility of the epi-spline estimation framework for study situations similar to this. As we discussed previously, we recognize that we are dealing with unique challenges to fully represent performance based on the small data samples. As we saw in Figure 4.2, the densities, and in particular their relationships to one another, did not always fit our intuition of how the results should change with increased exposure. For example, Figure 4.2 would lead you to believe that performance improves more dramatically after one hour of exposure than with no exposure, and that performance is degraded more significantly after two hours of exposure than after three hours.

These conclusions do not match qualitative information that the relationship between exposure time and the impact on performance should be essentially monotonic. That is, as exposure time increases, performance should decrease. But with only fifteen observations, it is very easy to

obtain estimates that contradict such qualitative information. This is where we can leverage the ability of the epi-spline estimation framework to incorporate soft information to achieve a better description of system performance.

Consider, then, the incorporation of an upper bound on the first moment, or mean, of the density estimate. Without discarding data observations as a support bound would potentially do, a bound on the mean requires the majority of the density's mass to reside in a particular region. With this constraint implemented in a progressive manner in the four exposure time cases, we can construct estimates that, in some sense, accomplish the qualitative relationship we believe is present between the true densities.

The "Data sample" column of Table 4.1 shows the sample means calculated directly from the fifteen data points in each case. The subsequent columns are the means calculated from the epi-spline estimates with the stated information. The four estimates with the bound on the first moment implemented are shown in Figure 4.3.

Table 4.1: Mean estimates of USMC HAT data.

	Data sample	Epi-Spline, unimodal	Epi-Spline, 1st moment bound added
no exposure	0.035687	0.035687	0.035687 (bound = 0.036)
1 hour exposure	0.091998	0.091997	0.035000 (bound = 0.035)
2 hour exposure	-0.027371	-0.027401	-0.027371 (bound = 0.035)
3 hour exposure	-0.070614	-0.070615	-0.070613 (bound = -0.027)

The sample mean in the control group, no exposure, is 0.035687. We place a relaxed bound on the first moment of 0.036 and find that the mean of the epi-spline estimate is unchanged, indicating that the constraint is not active. To implement the moment bounds in a progressive manner, we then use a slightly restrictive version of the control group mean, 0.035, as the upper bound on the 1 hour exposure estimate.

We see from Table 4.1 that, of the four exposure cases, the 1 hour exposure estimate is the most impacted by the upper bound on the first moment. The 1 hour exposure sample mean is 0.091998 and the mean of the epi-spline estimate with only the unimodal constraint is almost identical at 0.091997. However, with the first moment bound of 0.035 introduced, the estimate responds as we expect. Mass of the density is redistributed and the new estimate's mean is precisely 0.035, indicating that the constraint is active in the estimation problem. Note that

the location of the mode of the 1 hour exposure estimate does not change from the previous estimate shown in Figure 4.2, but the height of the density at the mode is reduced and the mass in the left tail increases.

We continue the same progressive implementation of the bounds on the mean with the 2 and 3 hour exposure cases. That is, we use the calculated mean of a given exposure case as the bound on the mean of the following case. For example, the final estimate for the 1 hour exposure case is 0.035, so this becomes the bound on the mean of the 2 hour exposure case. In both the 2 and 3 hour exposure cases, the bounds do not restrict the estimate and, thus, the means are essentially unchanged.
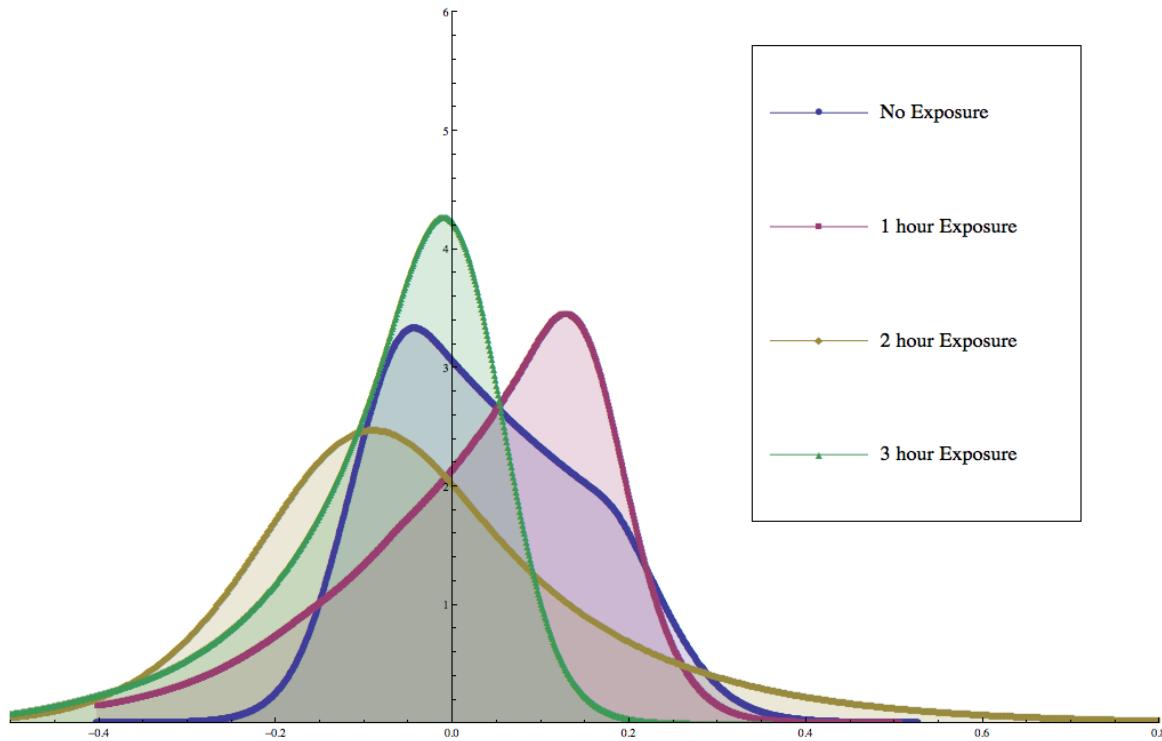
Figure 4.3: Density estimates of change in cognitive throughput based on waterborne exposure in EFV - cooled air configuration with unimodal constraint and progressive upper bounds on the 1st moment.

The constraint formulation used here to place bounds on the first moment is easily extendable to additional moments. For example, limits on the variability of a density can be implemented through bounds on the second moment.

The adjustment to the estimates as a result of the moment information available is significant. Consider that these probability density estimates will be used for random variate generation. For example, the estimates may be used to generate inputs for another system such as a computer simulation for evaluating potential vehicles for the USMC. The estimated probability densities are used to generate random variables as stochastic inputs to the simulation. The epi-spline estimates have the potential of more accurately representing the random variates because of their ability to utilize available soft information.

THIS PAGE INTENTIONALLY LEFT BLANK

CHAPTER 5:
CONCLUSION

This thesis deals with the problem of estimating system performance in a fully descriptive statistical manner when significant uncertainty is present, that is, we seek to quantify the uncertainty about the performance in an accurate and rigorous way. We propose the application of the epi-spline estimation framework for various uncertainty quantification contexts. In particular, we emphasize the flexibility of the epi-spline framework in its ability to systematically incorporate any soft information available in a given problem context to further enhance the accuracy of the estimate. We present results and analysis that clearly support the vast potential of the epi-spline framework in the area of UQ and nonparametric density estimation.

5.1   Key Findings

In the analytic cases presented in Chapter 3, we present empirical results that support the basic proposition that the epi-spline framework produces very reasonable estimates when compared to known probability densities. We also present results of how the epi-spline estimates compare to kernel estimates based on the same data sets. The epi-spline outperforms the kernel estimate in most of the benchmark cases that we examine based on MSE statistics.

We present epi-spline estimates from several analytic test cases where we can compare our estimates with the true output densities. Initially, we also illustrate the impact of the sample size on the estimates, which, along with the mathematical support provided in Chapter 2, indicates that the estimates approach the true density as the sample size goes to infinity.

Fifty random replications with samples of five observations and no soft information shows that the epi-spline has an average MSE almost 48% lower than the kernel estimates with a 96% reduction in standard deviation. A similar fifty replication test shows a reduction of over 23% in average MSE with an almost 88% decrease in standard deviation. Continuing analysis reveals that fifty random replications of the high information based epi-spline estimates further reduce the average MSE over the no soft information epi-spline estimates by upwards of 65% with a standard deviation reduction of another 56%.

The structural engineering column example illustrates the ability of the epi-spline framework to perform well under a more complex system function where we have multiple sources of uncer-

tainty in the input vector. We continue to see epi-spline estimates that significantly outperform those produced by a standard kernel estimator.

Lastly, we explore the application of the epi-spline framework to a current real-world research study context. We discuss the identification of sources of soft information and how they may or may not be appropriate in certain circumstances. We also discuss a novel method to address shortcomings in small data sets in order to produce estimates that more accurately represent the qualitative understanding of the problem context.

5.2 Future Research

There are several directions in which this thesis work can be expanded to complement the broader research effort. One primary expansion area is to move the empirical work to two-dimensional problem contexts where the system performance output ξ is no longer univariate, but represents a random vector of output measures. In the multivariate case, the elements of ξ may be correlated and this adds further complexity to the multidimensional estimation problem.

Another area of significant potential is the identification of additional sources of soft information from various problem contexts, particularly those with defense related applicability. The indentification of the sources of information as well as the constraint formulations that facilitate the incorporation of the information into the estimation problem is of vital importance. The unique strength of the epi-spline framework rests in its ability to leverage soft information for improved estimates.

Further research in how to best leverage current methods of gradient estimation in stochastic simulation would be particularly beneficial. Empirical results presented in this thesis make a strong argument for the potential of gradient information to improve density estimates. Simulation is an area of great potential for the application of the epi-spline framework in both output analysis and input generation. Many of the current gradient estimation techniques being researched are particularly applicable to the simulation context.

Lastly, there are significant opportunities to continue development and refinement of the numerical implementation of the estimation framework and information constraints. The epi-spline estimator is currently implemented in *Matlab*, but work in other languages could add value to the research effort and make the area more accessible to others in the community of interest.

LIST OF REFERENCES

[1] M. S. Eldred and L. P. Swiler, "Efficient algorithms for mixed aleatory-epistemic uncertainty quantification with application to radiation-hardened electronics; part 1: Algorithms and benchmark results," Tech. Rep. SAND2009-5805, Sandia National Laboratories, Albuquerque, NM, September 2009.

[2] J. Berger *et al.*, "ASA, SIAM collaborate on uncertainty quantification journal," *Amstat News*, p. 21, April 2012.

[3] ASME 2009 International Design Engineering Technical Conferences and 35th Design Automation Conference, *Reliable design optimization under aleatory and epistemic uncertainty*, August 2009.

[4] A. Chaidez *et al.*, "Final test report for the habitability assessment test (fouo)," Tech. Rep. AVTB-FTR-11-EFV-HAT-101, Amphibious Vehicle Test Branch, January 2012.

[5] M. S. Eldred, L. P. Swiler, and G. Tang, "Mixed aleatory-epistemic uncertainty quantification with stochastic expansions and optimization-based interval estimation," *Reliability Engineering and System Safety*, vol. 96, pp. 1092–1113, April 2011.

[6] E. Fix and J. L. Hodges, "Nonparametric discrimination: Consistency properties," report number 4, USAF School of Aviation Medicine, Randolph Field, TX, 1951.

[7] D. W. Scott, *Multivariate Density Estimation*. New York, NY: John Wiley and Sons, Inc., 1992.

[8] D. W. Scott, A. M. Gotto, J. S. Cole, and G. A. Gorry, "Plasma lipids as collateral risk factors in coronary artery disease: A study of 371 males with chest pain," *J. Chronic Diseases*, vol. 31, pp. 337–345, 1978.

[9] M. S. Casey and R. Wets, "Density estimation: Exploiting non-data information," *J. American Mathematical Association*, (submitted for publication) 2012.

[10] J. O. Royset, "Nonparametric density estimation: An optimization perspective." Presentation, West Coast Optimization Meeting, Seattle, WA, May 2012.

[11] T. Haukaas and A. D. Kiureghian, "Parameter sensitivity and importance measures in non-linear finite element reliability analysis," *J. Engineering Mechanics*, vol. 131, pp. 1013–1026, 2005.

[12] J. R. Thompson and R. A. Tapia, *Nonparametric Function Estimation, Modeling, and Simulation*. Philadelphia, PA: SIAM Publishers, 1990.

[13] M. C. Fu and J.-Q. Hu, *Conditional Monte Carlo - Gradient Estimation and Optimization Applications*. Norwell, MA: Kluwer Academic Publishers, 1997.

[14] B. Lee, "A field study of cognitive performance degradation among embarked infantry personnel exposed to waterborne motion," Master's thesis, Naval Postgraduate School, Monterey, CA, (to be published) 2012.

Initial Distribution List

1. Defense Technical Information Center
   Ft. Belvoir, Virginia

2. Dudly Knox Library
   Naval Postgraduate School
   Monterey, California

3. Associate Professor Johannes O. Royset
   Department of Operations Research
   Naval Postgraduate School
   Monterey, California

4. COL Scott T. Nestler, PhD
   Department of Operations Research
   Naval Postgraduate School
   Monterey, California

5. Distinguished Research Professor Roger J-B Wets
   Department of Mathematics
   University of California, Davis
   Davis, California

6. Professor Michael Fu
   Decision, Operations, and Information Technologies Department
   University of Maryland
   College Park, Maryland

7. TRADOC Analysis Center – Ft. Leavenworth
   Ft. Leavenworth, Kansas

8. LTC John Alt
   TRADOC Analysis Center – Monterey
   Monterey, California